

10

Superconductivity

EXPERIMENTAL SURVEY	259
Occurrence of superconductivity	260
Destruction of superconductivity by magnetic fields	262
Meissner effect	262
Heat capacity	264
Energy gap	266
Microwave and infrared properties	268
Isotope effect	269
THEORETICAL SURVEY	270
Thermodynamics of the superconducting transition	270
London equation	273
Coherence length	276
BCS theory of superconductivity	277
BCS ground state	278
Flux quantization in a superconducting ring	279
Duration of persistent currents	282
Type II superconductors	283
Vortex state	284
Estimation of H_{c1} and H_{c2}	284
Single particle tunneling	287
Josephson superconductor tunneling	289
Dc Josephson effect	289
Ac Josephson effect	290
Macroscopic quantum interference	292
HIGH-TEMPERATURE SUPERCONDUCTORS	293

NOTATION: In this chapter B_a denotes the applied magnetic field. In the CGS system the critical value B_{ac} of the applied field will be denoted by the symbol H_c in accordance with the custom of workers in superconductivity. Values of B_{ac} are given in gauss in CGS units and in teslas in SI units, with $1 \text{ T} = 10^4 \text{ G}$. In SI we have $B_{ac} = \mu_0 H_c$.

SUMMARY	294
PROBLEMS	294
1. Magnetic field penetration in a plate	294
2. Critical field of thin films	295
3. Two-fluid model of a superconductor	295
4. Structure of a vortex	295
5. London penetration depth	296
6. Diffraction effect of Josephson junction	296
7. Meissner effect in sphere	296
REFERENCE	296
APPENDICES RELEVANT TO SUPERCONDUCTIVITY	000
H Cooper Pairs	000
I Ginzburg-Landau Equation	000
J Electron-Phonon Collisions	000

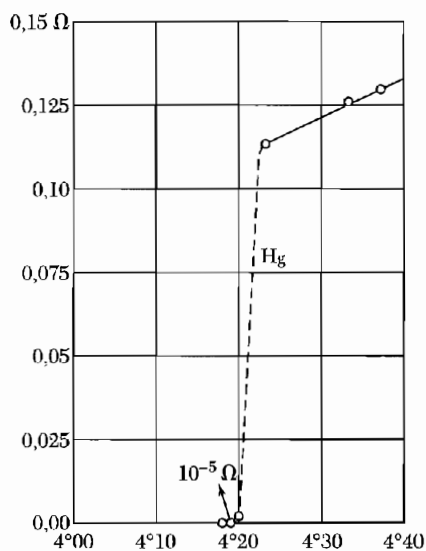


Figure 1 Resistance in ohms of a specimen of mercury versus absolute temperature. This plot by Kamerlingh Onnes marked the discovery of superconductivity.

CHAPTER 10: SUPERCONDUCTIVITY

The electrical resistivity of many metals and alloys drops suddenly to zero when the specimen is cooled to a sufficiently low temperature, often a temperature in the liquid helium range. This phenomenon, called superconductivity, was observed first by Kamerlingh Onnes in Leiden in 1911, three years after he first liquified helium. At a critical temperature T_c , the specimen undergoes a phase transition from a state of normal electrical resistivity to a superconducting state, Fig. 1.

Superconductivity is now very well understood. It is a field with many practical and theoretical aspects. The length of this chapter and the relevant appendices reflect the richness and subtleties of the field.

EXPERIMENTAL SURVEY

In the superconducting state the dc electrical resistivity is zero, or so close to zero that persistent electrical currents have been observed to flow without attenuation in superconducting rings for more than a year, until at last the experimentalist wearied of the experiment.

The decay of supercurrents in a solenoid was studied by File and Mills using precision nuclear magnetic resonance methods to measure the magnetic field associated with the supercurrent. They concluded that the decay time of the supercurrent is not less than 100,000 years. We estimate the decay time below. In some superconducting materials, particularly those used for superconducting magnets, finite decay times are observed because of an irreversible redistribution of magnetic flux in the material.

The magnetic properties exhibited by superconductors are as dramatic as their electrical properties. The magnetic properties cannot be accounted for by the assumption that a superconductor is a normal conductor with zero electrical resistivity.

It is an experimental fact that a bulk superconductor in a weak magnetic field will act as a perfect diamagnet, with zero magnetic induction in the interior. When a specimen is placed in a magnetic field and is then cooled through the transition temperature for superconductivity, the magnetic flux originally present is ejected from the specimen. This is called the **Meissner effect**. The sequence of events is shown in Fig. 2. The unique magnetic properties of superconductors are central to the characterization of the superconducting state.

The superconducting state is an ordered state of the conduction electrons of the metal. The order is in the formation of loosely associated pairs of electrons. The electrons are ordered at temperatures below the transition temperature, and they are disordered above the transition temperature.

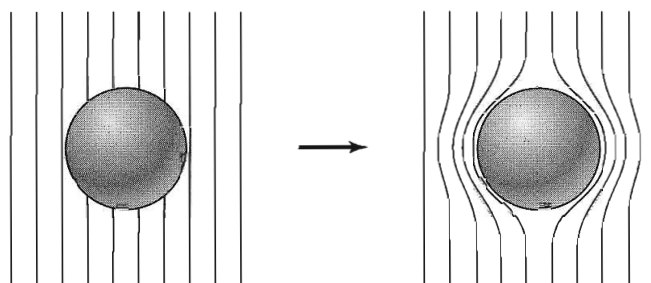


Figure 2 Meissner effect in a superconducting sphere cooled in a constant applied magnetic field; on passing below the transition temperature the lines of induction \mathbf{B} are ejected from the sphere.

The nature and origin of the ordering was explained by Bardeen, Cooper, and Schrieffer.¹ In the present chapter we develop as far as we can in an elementary way the physics of the superconducting state. We shall also discuss the basic physics of the materials used for superconducting magnets, but not their technology. Appendices H and I give deeper treatments of the superconducting state.

Occurrence of Superconductivity

Superconductivity occurs in many metallic elements of the periodic system and also in alloys, intermetallic compounds, and doped semiconductors. The range of transition temperatures best confirmed at present extends from 90.0 K for the compound $\text{YBa}_2\text{Cu}_3\text{O}_7$ to below 0.001 K for the element Rh. Several *f*-band superconductors, also known as “exotic superconductors,” are listed in Chapter 6. Several materials become superconducting only under high pressure; for example, Si has a superconducting form at 165 kbar, with $T_c = 8.3$ K. The elements known to be superconducting are displayed in Table 1, for zero pressure.

Will every nonmagnetic metallic element become a superconductor at sufficiently low temperatures? We do not know. In experimental searches for superconductors with ultralow transition temperatures it is important to eliminate from the specimen even trace quantities of foreign paramagnetic elements, because they can lower the transition temperature severely. One part of Fe in 10^4 will destroy the superconductivity of Mo, which when pure has $T_c = 0.92$ K; and 1 at. percent of gadolinium lowers the transition temperature of lanthanum from 5.6 K to 0.6 K. Nonmagnetic impurities have no very marked effect on the transition temperature. The transition temperatures of a number of interesting superconducting compounds are listed in Table 2. Several organic compounds show superconductivity at fairly low temperatures.

¹J. Bardeen, L. N. Cooper, and J. R. Schrieffer, *Phys. Rev.* **106**, 162 (1957); **108**, 1175 (1957).

Table 1 Superconductivity parameters of the elements

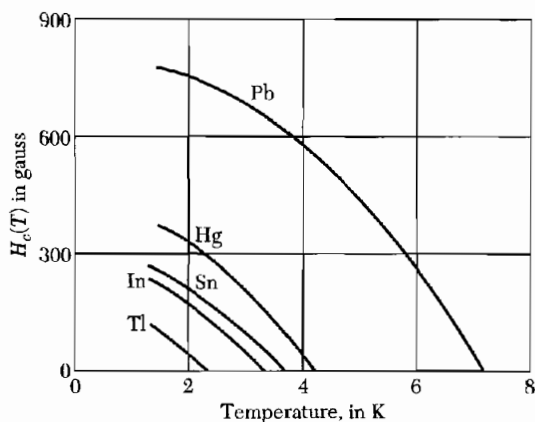
An asterisk denotes an element superconducting only in thin films or under high pressure in a crystal modification not normally stable. Data courtesy of B. T. Matthias, revised by T. Geballe.

Li		Be		B		C		N		O		F		Ne		
			0.026													
Na		Mg		Al		Si*		P*		S*		Cl		Ar		
						1.140										
Transition temperature in K																
Critical magnetic field at absolute zero in gauss (10 ⁻¹ tesla)																
K	Ca	Sc	Ti	V	Cr*	Mn	Fe	Co	Ni	Cu	Zn	Ga	Ge*	As*	Se*	Kr
			0.39	5.38							0.875	1.091				
			100	1420							53	51				
Rb	Sr	Y*	Zr	Nb	Mo	Tc	Ru	Rh	Pd	Ag	Cd	In	Sn ^(w)	Sb*	Te*	Xe
			0.546	9.50	0.92	7.77	0.51	.0003			0.56	3.4035	3.722			
			47	1980	95	1410	70	.049			30	293	309			
Cs*	Ba*	La _{fcc}	Hf	Ta	W	Re	Os	Ir	Pt	Au	Hg ^(v)	Tl	Pb	Bi*	Po	Rn
			6.00	4.483	0.012	1.4	0.655	0.14			4.153	2.39	7.193			
			1100	830	1.07	198	65	19			412	171	803			
Transition temperature in K																
Fr	Ra	Ac	Ce*	Pr	Nd	Pm	Sm	Eu	Gd	Tb	Dy	Ho	Er	Tm	Yb	Lu
																0.1
			Th	Pa	U*(α)	Np	Pu	Am	Cm	Bk	Cf	Es	Fm	Md	No	Lr
			1.368	1.4												
			1.62													

Table 2 Superconductivity of selected compounds

Compound	T_c in K	Compound	T_c in K
Nb ₃ Sn	18.05	V ₃ Ca	16.5
Nb ₃ Ge	23.2	V ₃ Si	17.1
Nb ₃ Al	17.5	YBa ₂ Cu ₃ O _{6.9}	90.0
NbN	16.0	Rb ₂ CsC ₆₀	31.3
C ₆₀	19.2	MgB ₂	39.0

Figure 3 Experimental threshold curves of the critical field $H_c(T)$ versus temperature for several superconductors. A specimen is superconducting below the curve and normal above the curve.



Destruction of Superconductivity by Magnetic Fields

A sufficiently strong magnetic field will destroy superconductivity. The threshold or critical value of the applied magnetic field for the destruction of superconductivity is denoted by $H_c(T)$ and is a function of the temperature. At the critical temperature the critical field is zero: $H_c(T_c) = 0$. The variation of the critical field with temperature for several superconducting elements is shown in Fig. 3.

The threshold curves separate the superconducting state in the lower left of the figure from the normal state in the upper right. Note: We should denote the critical value of the applied magnetic field as B_{ac} , but this is not common practice among workers in superconductivity. In the CGS system we shall always understand that $H_c \equiv B_{ac}$, and in the SI we have $H_c \equiv B_{ac}/\mu_0$. The symbol B_a denotes the applied magnetic field.

Meissner Effect

Meissner and Ochsenfeld (1933) found that if a superconductor is cooled in a magnetic field to below the transition temperature, then at the transition the lines of induction B are pushed out (Fig. 2). The Meissner effect shows that a bulk superconductor behaves as if $B = 0$ inside the specimen.

We obtain a particularly useful form of this result if we limit ourselves to long thin specimens with long axes parallel to B_a : now the demagnetizing field contribution (see Chapter 16) to B will be negligible, whence:²

$$\text{(CGS)} \quad B = B_a + 4\pi M = 0 ; \quad \text{or} \quad \frac{M}{B_a} = -\frac{1}{4\pi} ; \quad (1)$$

$$\text{(SI)} \quad B = B_a + \mu_0 M = 0 ; \quad \text{or} \quad \frac{M}{B_a} = -\frac{1}{\mu_0} = -\epsilon_0 c^2 .$$

The result $B = 0$ cannot be derived from the characterization of a superconductor as a medium of zero resistivity. From Ohm's law, $\mathbf{E} = \rho \mathbf{j}$, we see that if the resistivity ρ goes to zero while \mathbf{j} is held finite, then \mathbf{E} must be zero. By a Maxwell equation $d\mathbf{B}/dt$ is proportional to curl \mathbf{E} , so that zero resistivity implies $d\mathbf{B}/dt = 0$, but not $\mathbf{B} = 0$. This argument is not entirely transparent, but the result predicts that the flux through the metal cannot change on cooling through the transition. The Meissner effect suggests that perfect diamagnetism is an essential property of the superconducting state.

We expect another difference between a superconductor and a perfect conductor, defined as a conductor in which the electrons have an infinite mean free path. When the problem is solved in detail, it turns out that a perfect conductor when placed in a magnetic field cannot produce a permanent eddy current screen: the field will penetrate about 1 cm in an hour.³

The magnetization curve expected for a superconductor under the conditions of the Meissner-Ochsenfeld experiment is sketched in Fig. 4a. This applies quantitatively to a specimen in the form of a long solid cylinder placed in a longitudinal magnetic field. Pure specimens of many materials exhibit this behavior; they are called **type I superconductors** or, formerly, soft superconductors. The values of H_c are always too low for type I superconductors to have application in coils for superconducting magnets.

Other materials exhibit a magnetization curve of the form of Fig. 4b and are known as **type II superconductors**. They tend to be alloys (as in Fig. 5a) or transition metals with high values of the electrical resistivity in the normal state: that is, the electronic mean free path in the normal state is short. We shall see later why the mean free path is involved in the "magnetization" of superconductors.

Type II superconductors have superconducting electrical properties up to a field denoted by H_{c2} . Between the lower critical field H_{c1} and the upper critical field H_{c2} the flux density $B \neq 0$ and the Meissner effect is said to be incomplete. The value of H_{c2} may be 100 times or more higher (Fig. 5b) than

²Diamagnetism, the magnetization M , and the magnetic susceptibility are defined in Chapter 14. The magnitude of the apparent diamagnetic susceptibility of bulk superconductors is very much larger than in typical diamagnetic substances. In (1), M is the magnetization equivalent to the superconducting currents in the specimen.

³A. B. Pippard, *Dynamics of conduction electrons*, Gordon and Breach, 1965.

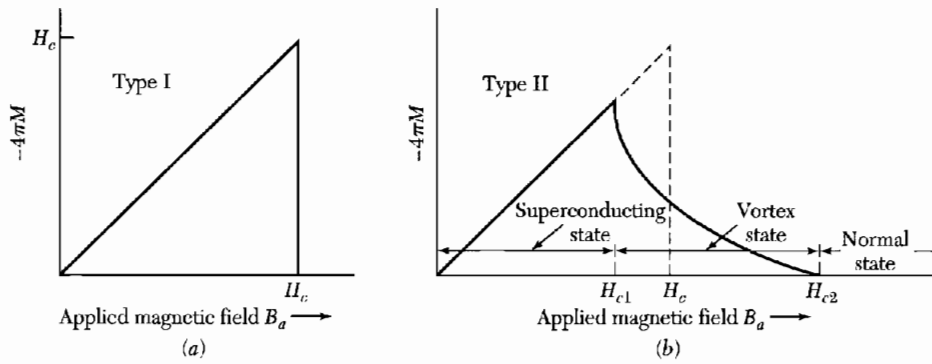


Figure 4 (a) Magnetization versus applied magnetic field for a bulk superconductor exhibiting a complete Meissner effect (perfect diamagnetism). A superconductor with this behavior is called a type I superconductor. Above the critical field H_c the specimen is a normal conductor and the magnetization is too small to be seen on this scale. Note that minus $4\pi M$ is plotted on the vertical scale: the negative value of M corresponds to diamagnetism. (b) Superconducting magnetization curve of a type II superconductor. The flux starts to penetrate the specimen at a field H_{c1} lower than the thermodynamic critical field H_c . The specimen is in a vortex state between H_{c1} and H_{c2} , and it has superconducting electrical properties up to H_{c2} . Above H_{c2} the specimen is a normal conductor in every respect, except for possible surface effects. For given H_c the area under the magnetization curve is the same for a type II superconductor as for a type I. (CGS units in all parts of this figure.)

the value of the critical field H_c calculated from the thermodynamics of the transition. In the region between H_{c1} and H_{c2} the superconductor is threaded by flux lines and is said to be in the **vortex state**. A field H_{c2} of 410 kG (41 teslas) has been attained in an alloy of Nb, Al, and Ge at the boiling point of helium, and 540 kG (54 teslas) has been reported for PbMo_6S_8 .

Commercial solenoids wound with a hard superconductor produce high steady fields over 100 kG. A “hard superconductor” is a type II superconductor with a large magnetic hysteresis, usually induced by mechanical treatment. Such materials have an important medical application in magnetic resonance imaging (MRI).

Heat Capacity

In all superconductors the entropy decreases markedly on cooling below the critical temperature T_c . Measurements for aluminum are plotted in Fig. 6. The decrease in entropy between the normal state and the superconducting state tells us that the superconducting state is more ordered than the normal state, for the entropy is a measure of the disorder of a system. Some or all of the electrons thermally excited in the normal state are ordered in the superconducting state. The change in entropy is small, in aluminum of the order of $10^{-4} k_B$ per atom. The small entropy change must mean that only a small fraction (of the order of 10^{-4}) of the conduction electrons participate in the transition to the ordered superconducting state. The free energies of normal and superconducting states are compared in Fig. 7.

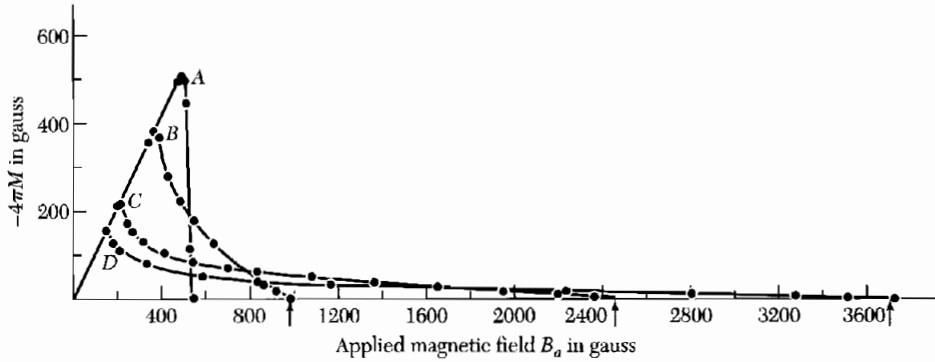


Figure 5a Superconducting magnetization curves of annealed polycrystalline lead and lead-indium alloys at 4.2 K. (A) lead; (B) lead-2.08 wt. percent indium; (C) lead-8.23 wt. percent indium; (D) lead-20.4 wt. percent indium. (After Livingston.)

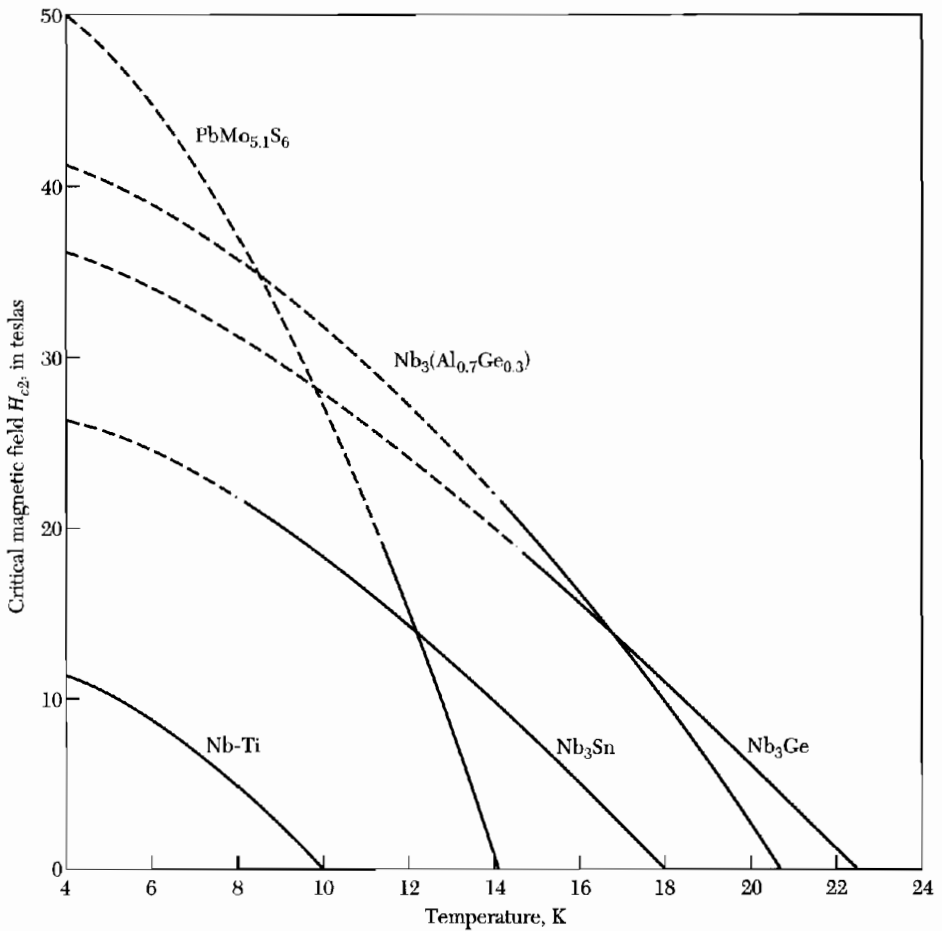


Figure 5b Strong magnetic fields are within the capability of certain Type II materials.

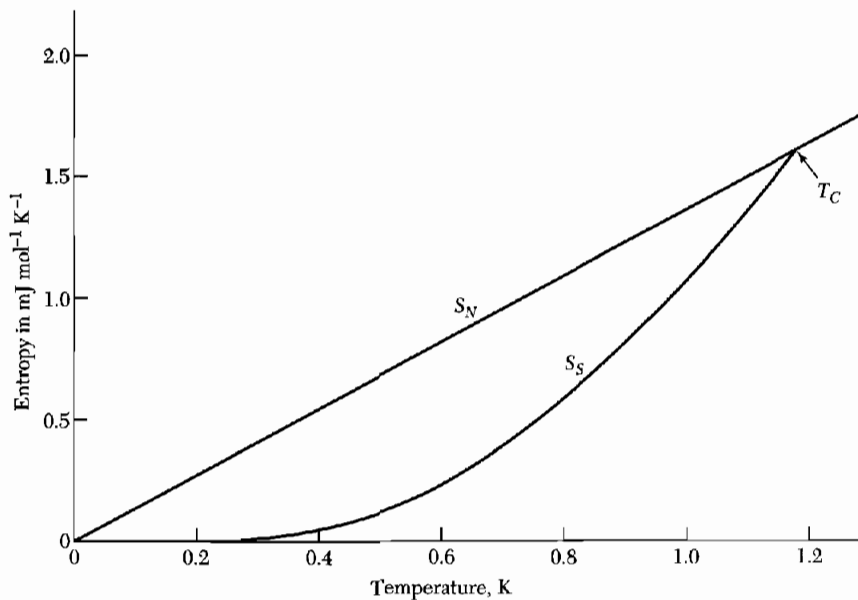


Figure 6 Entropy S of aluminum in the normal and superconducting states as a function of the temperature. The entropy is lower in the superconducting state because the electrons are more ordered here than in the normal state. At any temperature below the critical temperature T_c the specimen can be put in the normal state by application of a magnetic field stronger than the critical field.

The heat capacity of gallium is plotted in Fig. 8: (a) compares the normal and superconducting states; (b) shows that the electronic contribution to the heat capacity in the superconducting state is an exponential form with an argument proportional to $-1/T$, suggestive of excitation of electrons across an energy gap. An energy gap (Fig. 9) is a characteristic, but not universal, feature of the superconducting state. The gap is accounted for by the Bardeen-Cooper-Schrieffer (BCS) theory of superconductivity (see Appendix H).

Energy Gap

The energy gap of superconductors is of entirely different origin and nature than the energy gap of insulators. In an insulator the energy gap is caused by the electron-lattice interaction, Chapter 7. This interaction ties the electrons to the lattice. In a superconductor the important interaction is the electron-electron interaction which orders the electrons in \mathbf{k} space with respect to the Fermi gas of electrons.

The argument of the exponential factor in the electronic heat capacity of a superconductor is found to be $-E_g/2k_B T$ and not $-E_g/k_B T$. This has been learnt from comparison with optical and electron tunneling determinations of the gap E_g . Values of the gap in several superconductors are given in Table 3.

The transition in zero magnetic field from the superconducting state to the normal state is observed to be a second-order phase transition. At a

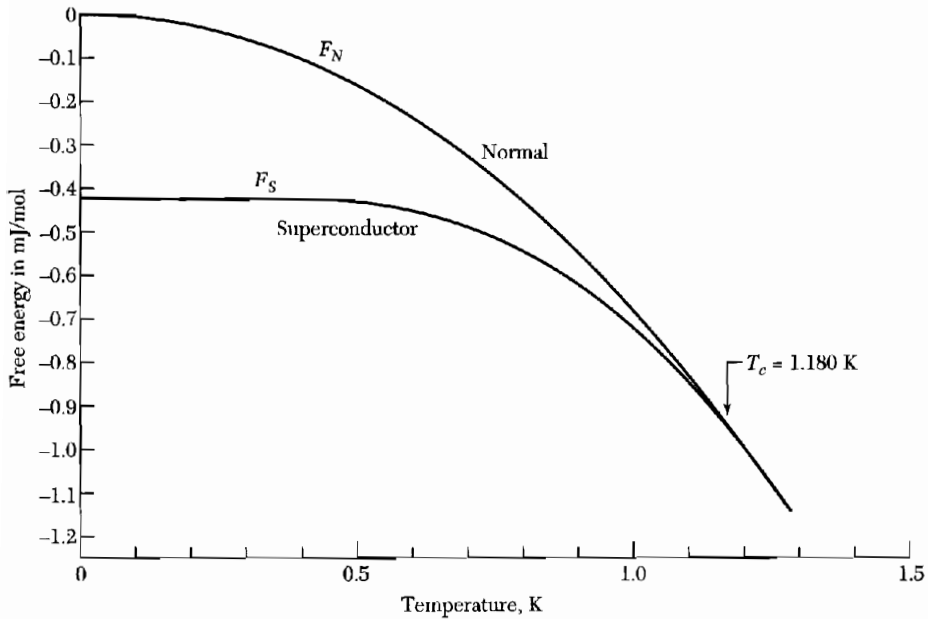


Figure 7 Experimental values of the free energy as a function of temperature for aluminum in the superconducting state and in the normal state. Below the transition temperature $T_c = 1.180$ K the free energy is lower in the superconducting state. The two curves merge at the transition temperature, so that the phase transition is second order (there is no latent heat of transition at T_c). The curve F_S is measured in zero magnetic field, and F_N is measured in a magnetic field sufficient to put the specimen in the normal state. (Courtesy of N. E. Phillips.)

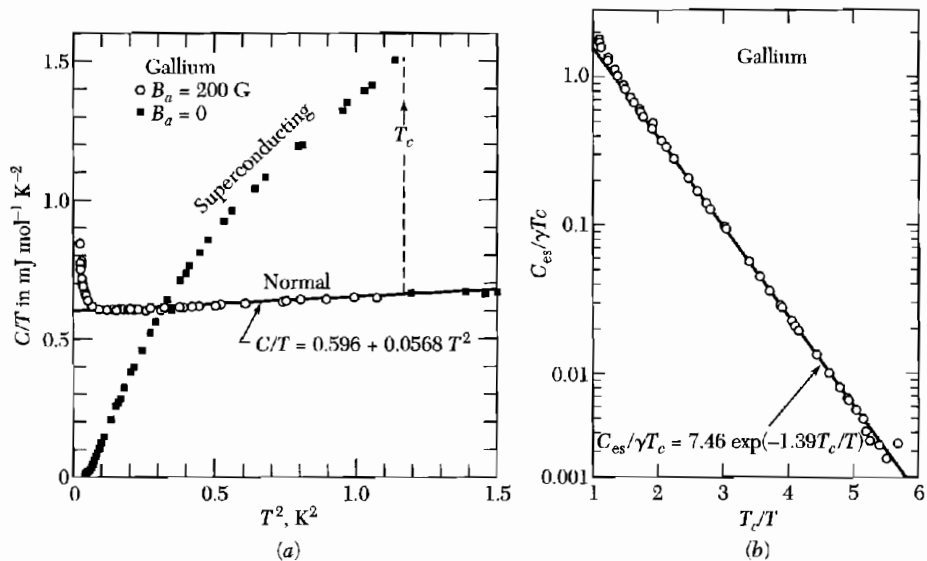


Figure 8 (a) The heat capacity of gallium in the normal and superconducting states. The normal state (which is restored by a 200 G field) has electronic, lattice, and (at low temperatures) nuclear quadrupole contributions. In (b) the electronic part C_{es} of the heat capacity in the superconducting state is plotted on a log scale versus T_c/T ; the exponential dependence on $1/T$ is evident. Here $\gamma = 0.60$ mJ mol⁻¹ deg⁻². (After N. E. Phillips.)

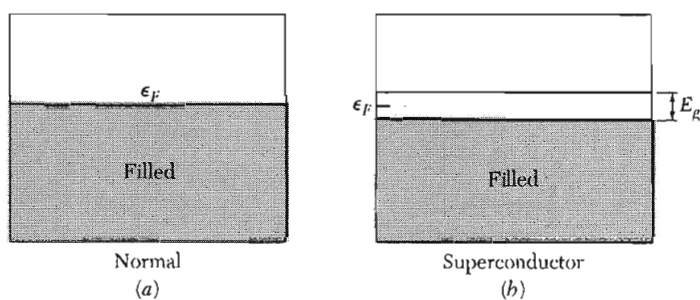


Figure 9 (a) Conduction band in the normal state; (b) energy gap at the Fermi level in the superconducting state. Electrons in excited states above the gap behave as normal electrons in rf fields: they cause resistance; at dc they are shorted out by the superconducting electrons. The gap E_g is exaggerated in the figure: typically $E_g \sim 10^{-4} \epsilon_F$.

Table 3 Energy gaps in superconductors, at $T = 0$

											Al	Si
$E_g(0)$ in 10^{-4} eV.											3.4	
$E_g(0)/k_B T_c$.											3.3	
Sc	Ti	V	Cr	Mn	Fe	Co	Ni	Cu	Zn	Ga	Ge	
		16.							2.4	3.3		
		3.4							3.2	3.5		
Y	Zr	Nb	Mo	Tc	Ru	Rh	Pd	Ag	Cd	In	Sn (w)	
		30.5	2.7						1.5	10.5	11.5	
		3.80	3.4						3.2	3.6	3.5	
La fcc	Hf	Ta	W	Re	Os	Ir	Pt	Au	Hg (n)	Tl	Pb	
19.		14.							16.5	7.35	27.3	
3.7		3.60							4.6	3.57	4.38	

second-order transition there is no latent heat, but there is a discontinuity in the heat capacity, evident in Fig. 8a. Further, the energy gap decreases continuously to zero as the temperature is increased to the transition temperature T_c , as in Fig. 10. A first-order transition would be characterized by a latent heat and by a discontinuity in the energy gap.

Microwave and Infrared Properties

The existence of an energy gap means that photons of energy less than the gap energy are not absorbed. Nearly all the photons incident are reflected as for any metal because of the impedance mismatch at the boundary between vacuum and metal, but for a very thin ($\sim 20 \text{ \AA}$) film more photons are transmitted in the superconducting state than in the normal state.

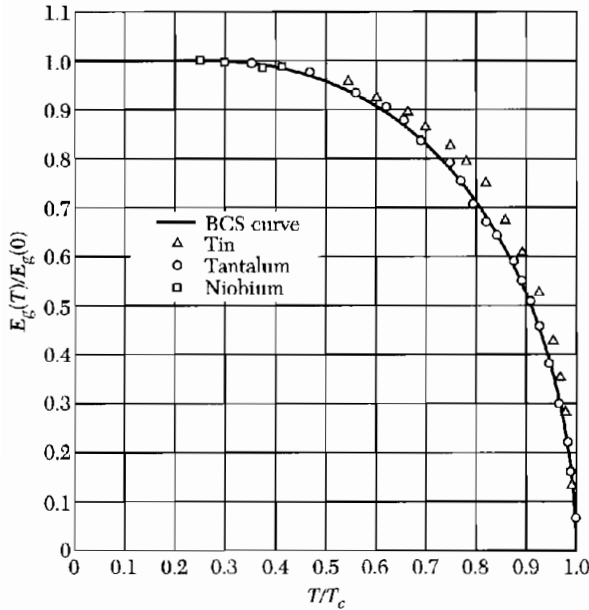


Figure 10 Reduced values of the observed energy gap $E_g(T)/E_g(0)$ as a function of the reduced temperature T/T_c , after Townsend and Sutton. The solid curve is drawn for the BCS theory.

For photon energies less than the energy gap, the resistivity of a superconductor vanishes at absolute zero. At $T \ll T_c$ the resistance in the superconducting state has a sharp threshold at the gap energy. Photons of lower energy see a resistanceless surface. Photons of higher energy than the energy gap see a resistance that approaches that of the normal state because such photons cause transitions to unoccupied normal energy levels above the gap.

As the temperature is increased not only does the gap decrease in energy, but the resistivity for photons with energy below the gap energy no longer vanishes, except at zero frequency. At zero frequency the superconducting electrons short-circuit any normal electrons that have been thermally excited above the gap. At finite frequencies the inertia of the superconducting electrons prevents them from completely screening the electric field, so that thermally excited normal electrons now can absorb energy (Problem 3).

Isotope Effect

It has been observed that the critical temperature of superconductors varies with isotopic mass. In mercury T_c varies from 4.185 K to 4.146 K as the average atomic mass M varies from 199.5 to 203.4 atomic mass units. The transition temperature changes smoothly when we mix different isotopes of the same element. The experimental results within each series of isotopes may be fitted by a relation of the form

$$M^\alpha T_c = \text{constant} . \quad (2)$$

Observed values of α are given in Table 4.

Table 4 Isotope effect in superconductorsExperimental values of α in $M^\alpha T_c = \text{constant}$, where M is the isotopic mass.

Substance	α	Substance	α
Zn	0.45 ± 0.05	Ru	0.00 ± 0.05
Cd	0.32 ± 0.07	Os	0.15 ± 0.05
Sn	0.47 ± 0.02	Mo	0.33
Hg	0.50 ± 0.03	Nb ₃ Sn	0.08 ± 0.02
Pb	0.49 ± 0.02	Zr	0.00 ± 0.05

From the dependence of T_c on the isotopic mass we learn that lattice vibrations and hence electron-lattice interactions are deeply involved in superconductivity. This was a fundamental discovery: there is no other reason for the superconducting transition temperature to depend on the number of neutrons in the nucleus.

The original BCS model gave the result $T_c \propto \theta_{\text{Debye}} \propto M^{-1/2}$, so that $\alpha = \frac{1}{2}$ in (2), but the inclusion of coulomb interactions between the electrons changes the relation. Nothing is sacred about $\alpha = \frac{1}{2}$. The absence of an isotope effect in Ru and Zr has been accounted for in terms of the electron band structure of these metals.

THEORETICAL SURVEY

A theoretical understanding of the phenomena associated with superconductivity has been reached in several ways. Certain results follow directly from thermodynamics. Many important results can be described by phenomenological equations: the London equations and the Landau-Ginzburg equations (Appendix 1). A successful quantum theory of superconductivity was given by Bardeen, Cooper, and Schrieffer, and has provided the basis for subsequent work. Josephson and Anderson discovered the importance of the phase of the superconducting wavefunction.

Thermodynamics of the Superconducting Transition

The transition between the normal and superconducting states is thermodynamically reversible, just as the transition between liquid and vapor phases of a substance is reversible. Thus we may apply thermodynamics to the transition, and we thereby obtain an expression for the entropy difference between normal and superconducting states in terms of the critical field curve H_c versus T . This is analogous to the vapor pressure equation for the liquid-gas coexistence curve (*TP*, Chapter 10).

We treat a type I superconductor with a complete Meissner effect, so that $B = 0$ inside the superconductor. We shall see that the critical field H_c is a quantitative measure of the free energy difference between the superconducting and normal states at constant temperature. The symbol H_c will always refer to a bulk specimen, never to a thin film. For type II superconductors, H_c is understood to be the thermodynamic critical field related to the stabilization free energy.

The stabilization free energy of the superconducting state with respect to the normal state can be determined by calorimetric or magnetic measurements. In the calorimetric method the heat capacity is measured as a function of temperature for the superconductor and for the normal conductor, which means the superconductor in a magnetic field larger than H_c . From the difference of the heat capacities we can compute the free energy difference, which is the stabilization free energy of the superconducting state.

In the magnetic method the stabilization free energy is found from the value of the applied magnetic field that will destroy the superconducting state, at constant temperature. The argument follows. Consider the work done (Fig. 11) on a superconductor when it is brought reversibly at constant temperature from a position at infinity (where the applied field is zero) to a position \mathbf{r} in the field of a permanent magnet:

$$W = - \int_0^{B_a} \mathbf{M} \cdot d\mathbf{B}_a, \tag{3}$$

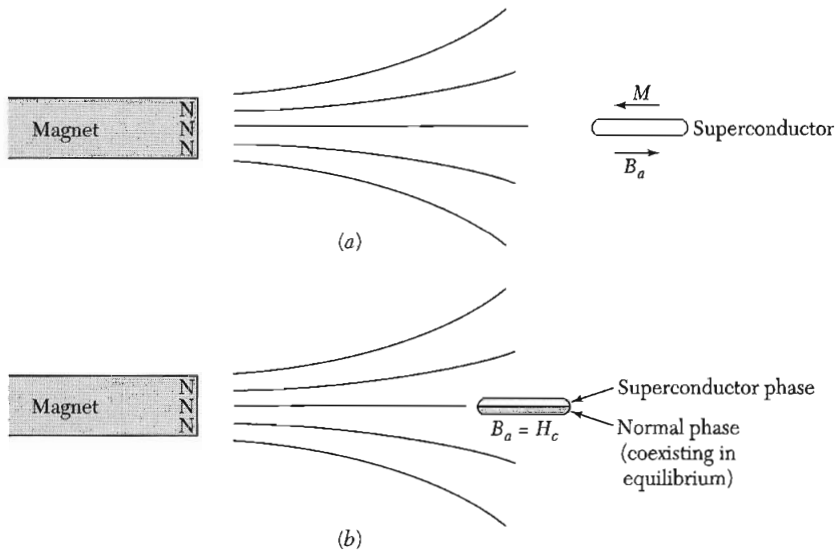


Figure 11 (a) A superconductor in which the Meissner effect is complete has $B = 0$, as if the magnetization were $M = -B_a/4\pi$, in CGS units. (b) When the applied field reaches the value B_{ac} , the normal state can coexist in equilibrium with the superconducting state. In coexistence the free energy densities are equal: $F_N(T, B_{ac}) = F_S(T, B_{ac})$.

per unit volume of specimen. This work appears in the energy of the magnetic field. The thermodynamic identity for the process is

$$dF = -\mathbf{M} \cdot d\mathbf{B}_a, \quad (4)$$

as in *TP*, Chapter 8.

For a superconductor with \mathbf{M} related to \mathbf{B}_a by (1) we have

$$\text{(CGS)} \quad dF_S = \frac{1}{4\pi} B_a dB_a; \quad (5)$$

$$\text{(SI)} \quad dF_S = \frac{1}{\mu_0} B_a dB_a.$$

The increase in the free energy density of the superconductor is

$$\text{(CGS)} \quad F_S(B_a) - F_S(0) = B_a^2/8\pi; \quad (6)$$

$$\text{(SI)} \quad F_S(B_a) - F_S(0) = B_a^2/2\mu_0,$$

on being brought from a position where the applied field is zero to a position where the applied field is B_a .

Now consider a normal nonmagnetic metal. If we neglect the small susceptibility⁴ of a metal in the normal state, then $M = 0$ and the energy of the normal metal is independent of field. At the critical field we have

$$F_N(B_{ac}) = F_N(0). \quad (7)$$

The results (6) and (7) are all we need to determine the stabilization energy of the superconducting state at absolute zero. At the critical value B_{ac} of the applied magnetic field the energies are equal in the normal and superconducting states:

$$\text{(CGS)} \quad F_N(B_{ac}) = F_S(B_{ac}) = F_S(0) + B_{ac}^2/8\pi, \quad (8)$$

$$\text{(SI)} \quad F_N(B_{ac}) = F_S(B_{ac}) = F_S(0) + B_{ac}^2/2\mu_0,$$

In SI units $H_c \equiv B_{ac}/\mu_0$, whereas in CGS units $H_c \equiv B_{ac}$.

The specimen is stable in either state when the applied field is equal to the critical field. Now by (7) it follows that

$$\text{(CGS)} \quad \Delta F \equiv F_N(0) - F_S(0) = B_{ac}^2/8\pi, \quad (9)$$

⁴This is an adequate assumption for type I superconductors. In type II superconductors in high fields the change in spin paramagnetism of the conduction electrons lowers the energy of the normal phase significantly. In some, but not all, type II superconductors the upper critical field is limited by this effect. Clogston has suggested that $H_{c2}(\text{max}) = 18,400 T_c$, where H_{c2} is in gauss and T_c in K.

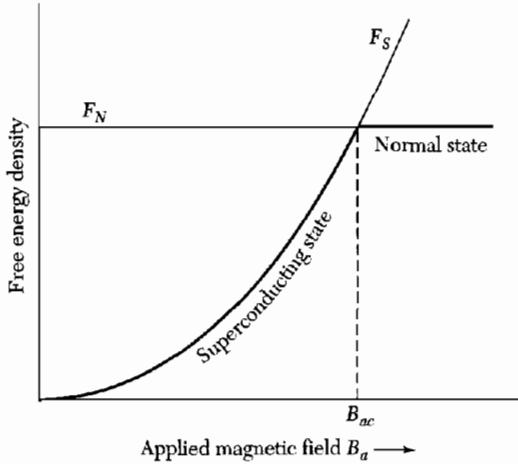


Figure 12 The free energy density F_N of a nonmagnetic normal metal is approximately independent of the intensity of the applied magnetic field B_a . At a temperature $T < T_c$ the metal is a superconductor in zero magnetic field, so that $F_S(T, 0)$ is lower than $F_N(T, 0)$. An applied magnetic field increases F , by $B_a^2/8\pi$, in CGS units, so that $F_S(T, B_a) = F_S(T, 0) + B_a^2/8\pi$. If B_a is larger than the critical field B_{ac} the free energy density is lower in the normal state than in the superconducting state, and now the normal state is the stable state. The origin of the vertical scale in the drawing is at $F_S(T, 0)$. The figure equally applies to U_S and U_N at $T = 0$.

where ΔF is the stabilization free energy density of the superconducting state. For aluminum, B_{ac} at absolute zero is 105 gauss, so that at absolute zero $\Delta F = (105)^2/8\pi = 439 \text{ erg cm}^{-3}$, in excellent agreement with the result of thermal measurements, 430 erg cm^{-3} .

At a finite temperature the normal and superconducting phases are in equilibrium when the magnetic field is such that their free energies $F = U - TS$ are equal. The free energies of the two phases are sketched in Fig. 12 as a function of the magnetic field. Experimental curves of the free energies of the two phases for aluminum are shown in Fig. 7. Because the slopes dF/dT are equal at the transition temperature, there is no latent heat at T_c .

London Equation

We saw that the Meissner effect implies a magnetic susceptibility $\chi = -1/4\pi$ in CGS in the superconducting state or, in SI, $\chi = -1$. Can we modify a constitutive equation of electrodynamics (such as Ohm's law) in some way to obtain the Meissner effect? We do not want to modify the Maxwell equations themselves. Electrical conduction in the normal state of a metal is described by Ohm's law $\mathbf{j} = \sigma \mathbf{E}$. We need to modify this drastically to describe conduction and the Meissner effect in the superconducting state. Let us make a *postulate* and see what happens.

We postulate that in the superconducting state the current density is directly proportional to the vector potential \mathbf{A} of the local magnetic field, where $\mathbf{B} = \text{curl } \mathbf{A}$. The gauge of \mathbf{A} will be specified. In CGS units we write the constant of proportionality as $-c/4\pi\lambda_L^2$ for reasons that will become clear.

Here c is the speed of light and λ_L is a constant with the dimensions of length. In SI units we write $-1/\mu_0\lambda_L^2$. Thus

$$\text{(CGS)} \quad \mathbf{j} = -\frac{c}{4\pi\lambda_L^2} \mathbf{A} ; \quad \text{(SI)} \quad \mathbf{j} = -\frac{1}{\mu_0\lambda_L^2} \mathbf{A} . \quad (10)$$

This is the London equation. We express it another way by taking the curl of both sides to obtain

$$\text{(CGS)} \quad \text{curl } \mathbf{j} = -\frac{c}{4\pi\lambda_L^2} \mathbf{B} ; \quad \text{(SI)} \quad \text{curl } \mathbf{j} = -\frac{1}{\mu_0\lambda_L^2} \mathbf{B} . \quad (11)$$

The London equation (10) is understood to be written with the vector potential in the London gauge in which $\text{div } \mathbf{A} = 0$, and $\mathbf{A}_n = 0$ on any external surface through which no external current is fed. The subscript n denotes the component normal to the surface. Thus $\text{div } \mathbf{j} = 0$ and $\mathbf{j}_n = 0$, the actual physical boundary conditions. The form (10) applies to a simply connected superconductor; additional terms may be present in a ring or cylinder, but (11) holds true independent of geometry.

First we show that the London equation leads to the Meissner effect. By a Maxwell equation we know that

$$\text{(CGS)} \quad \text{curl } \mathbf{B} = \frac{4\pi}{c} \mathbf{j} ; \quad \text{(SI)} \quad \text{curl } \mathbf{B} = \mu_0 \mathbf{j} ; \quad (12)$$

under static conditions. We take the curl of both sides to obtain

$$\text{(CGS)} \quad \text{curl curl } \mathbf{B} = -\nabla^2 \mathbf{B} = \frac{4\pi}{c} \text{curl } \mathbf{j} ;$$

$$\text{(SI)} \quad \text{curl curl } \mathbf{B} = -\nabla^2 \mathbf{B} = \mu_0 \text{curl } \mathbf{j} ;$$

which may be combined with the London equation (11) to give for a superconductor

$$\nabla^2 \mathbf{B} = \mathbf{B}/\lambda_L^2 . \quad (13)$$

This equation is seen to account for the Meissner effect because it does not allow a solution uniform in space, so that a uniform magnetic field cannot exist in a superconductor. That is, $\mathbf{B}(\mathbf{r}) = \mathbf{B}_0 = \text{constant}$ is not a solution of (13) unless the constant field \mathbf{B}_0 is identically zero. The result follows because $\nabla^2 \mathbf{B}_0$ is always zero, but \mathbf{B}_0/λ_L^2 is not zero unless \mathbf{B}_0 is zero. Note further that (12) ensures that $\mathbf{j} = 0$ in a region where $\mathbf{B} = 0$.

In the pure superconducting state the only field allowed is exponentially damped as we go in from an external surface. Let a semi-infinite superconductor

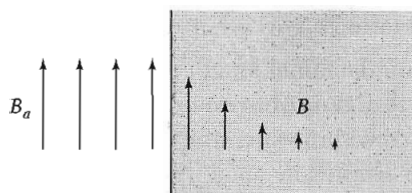


Figure 13 Penetration of an applied magnetic field into a semi-infinite superconductor. The penetration depth λ is defined as the distance in which the field decreases by the factor e^{-1} . Typically, $\lambda \approx 500 \text{ \AA}$ in a pure superconductor.

occupy the space on the positive side of the x axis, as in Fig. 13. If $B(0)$ is the field at the plane boundary, then the field inside is

$$B(x) = B(0) \exp(-x/\lambda_L) \quad (14)$$

for this is a solution of (13). In this example the magnetic field is assumed to be parallel to the boundary. Thus we see λ_L measures the depth of penetration of the magnetic field; it is known as the **London penetration depth**. Actual penetration depths are not described precisely by λ_L alone, for the London equation is now known to be somewhat oversimplified. It is shown by comparison of (22) with (11) that

$$\text{(CGS)} \quad \lambda_L = (mc^2/4\pi nq^2)^{1/2}; \quad \text{(SI)} \quad \lambda_L = (\epsilon_0 mc^2/nq^2)^{1/2} \quad (14a)$$

for particles of charge q and mass m in concentration n . Values are given in Table 5.

An applied magnetic field B_a will penetrate a thin film fairly uniformly if the thickness is much less than λ_L ; thus in a thin film the Meissner effect is not complete. In a thin film the induced field is much less than B_a , and there is little effect of B_a on the energy density of the superconducting state, so that (6) does not apply. It follows that the critical field H_c of thin films in parallel magnetic fields will be very high.

Table 5 Calculated intrinsic coherence length and London penetration depth, at absolute zero

Metal	Intrinsic Pippard coherence length ξ_0 , in 10^{-6} cm	London penetration depth λ_L , in 10^{-6} cm	λ_L/ξ_0
Sn	23.	3.4	0.16
Al	160.	1.6	0.010
Pb	8.3	3.7	0.45
Cd	76.	11.0	0.14
Nb	3.8	3.9	1.02

After R. Meservey and B. B. Schwartz.

Coherence Length

The London penetration depth λ_L is a fundamental length that characterizes a superconductor. An independent length is the **coherence length** ξ . The coherence length is a measure of the distance within which the superconducting electron concentration cannot change drastically in a spatially-varying magnetic field.

The London equation is a *local* equation: it relates the current density at a point \mathbf{r} to the vector potential at the same point. So long as $\mathbf{j}(\mathbf{r})$ is given as a constant time $\mathbf{A}(\mathbf{r})$, the current is required to follow exactly any variation in the vector potential. But the coherence length ξ is a measure of the range over which we should average \mathbf{A} to obtain \mathbf{j} . It is also a measure of the minimum spatial extent of a transition layer between normal and superconductor. The coherence length is best introduced into the theory through the Landau-Ginzburg equations, Appendix I. Now we give a plausibility argument for the energy required to modulate the superconducting electron concentration.

Any spatial variation in the state of an electronic system requires extra kinetic energy. A modulation of an eigenfunction increases the kinetic energy because the modulation will increase the integral of $d^2\varphi/dx^2$. It is reasonable to restrict the spatial variation of $\mathbf{j}(\mathbf{r})$ in such a way that the extra energy is less than the stabilization energy of the superconducting state.

We compare the plane wave $\psi(x) = e^{ikx}$ with the strongly modulated wavefunction:

$$\varphi(x) = 2^{-1/2} (e^{i(k+q)x} + e^{ikx}) . \quad (15a)$$

The probability density associated with the plane wave is uniform in space: $\psi^*\psi = e^{-ikx} e^{ikx} = 1$, whereas $\varphi^*\varphi$ is modulated with the wavevector q :

$$\begin{aligned} \varphi^*\varphi &= \frac{1}{2}(e^{-i(k+q)x} + e^{-ikx})(e^{i(k+q)x} + e^{ikx}) \\ &= \frac{1}{2}(2 + e^{iqx} + e^{-iqx}) = 1 + \cos qx . \end{aligned} \quad (15b)$$

The kinetic energy of the wave $\psi(x)$ is $\epsilon = \hbar^2 k^2/2m$; the kinetic energy of the modulated density distribution is higher, for

$$\int dx \varphi^* \left(-\frac{\hbar^2}{2m} \frac{d^2}{dx^2} \right) \varphi = \frac{1}{2} \left(\frac{\hbar^2}{2m} \right) [(k+q)^2 + k^2] \equiv \frac{\hbar^2}{2m} k^2 + \frac{\hbar^2}{2m} kq ,$$

where we neglect q^2 for $q \ll k$.

The increase of energy required to modulate is $\hbar^2 kq/2m$. If this increase exceeds the energy gap E_g , superconductivity will be destroyed. The critical value q_0 of the modulation wavevector is given by

$$\frac{\hbar^2}{2m} k q_0 = E_g . \quad (16a)$$

We define an **intrinsic coherence length** ξ_0 related to the critical modulation by $\xi_0 = 1/q_0$. We have

$$\xi_0 = \hbar^2 k_F / 2mE_g = \hbar v_F / 2E_g, \quad (16b)$$

where v_F is the electron velocity at the Fermi surface. On the BCS theory a similar result is found:

$$\xi_0 = 2\hbar v_F / \pi E_g. \quad (17)$$

Calculated values of ξ_0 from (17) are given in Table 5. The intrinsic coherence length ξ_0 is characteristic of a pure superconductor.

In impure materials and in alloys the coherence length ξ is shorter than ξ_0 . This may be understood qualitatively: in impure material the electron eigenfunctions already have wiggles in them: we can construct a given localized variation of current density with less energy from wavefunctions with wiggles than from smooth wavefunctions.

The coherence length first appeared in the Landau-Ginzburg equations; these equations also follow from the BCS theory. They describe the structure of the transition layer between normal and superconducting phases in contact. The coherence length and the actual penetration depth λ depend on the mean free path ℓ of the electrons measured in the normal state; the relationships are indicated in Fig. 14. When the superconductor is very impure, with a very small ℓ , then $\xi \approx (\xi_0 \ell)^{1/2}$ and $\lambda \approx \lambda_L (\xi_0 / \ell)^{1/2}$, so that $\lambda / \xi \approx \lambda_L / \ell$. This is the “dirty superconductor” limit. The ratio λ / ξ is denoted by κ .

BCS Theory of Superconductivity

The basis of a quantum theory of superconductivity was laid by the classic 1957 papers of Bardeen, Cooper, and Schrieffer. There is a “BCS theory of superconductivity” with a very wide range of applicability, from He³ atoms in their condensed phase, to type I and type II metallic superconductors, and to high-temperature superconductors based on planes of cuprate ions. Further,

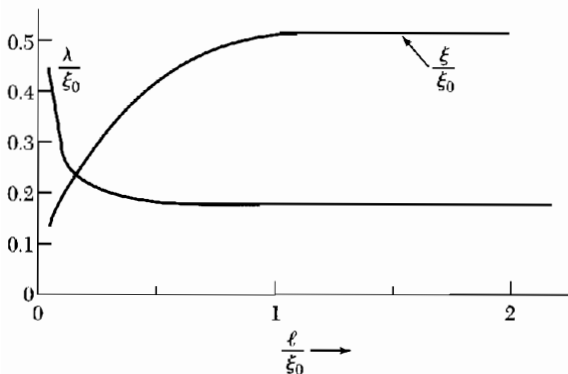


Figure 14 Penetration depth λ and the coherence length ξ as functions of the mean free path ℓ of the conduction electrons in the normal state. All lengths are in units of ξ_0 , the intrinsic coherence length. The curves are sketched for $\xi_0 = 10\lambda_L$. For short mean free paths the coherence length becomes shorter and the penetration depth becomes longer. The increase in the ratio $\kappa\lambda/\xi$ favors type II superconductivity.

there is a “BCS wavefunction” composed of particle pairs $\mathbf{k}\uparrow$ and $-\mathbf{k}\downarrow$, which, when treated by the BCS theory, gives the familiar electronic superconductivity observed in metals and exhibits the energy gaps of Table 3. This pairing is known as *s*-wave pairing. There are other forms of particle pairing possible with the BCS theory, but we do not have to consider other than the BCS wavefunction here. In this chapter we treat the specific accomplishments of BCS theory with a BCS wavefunction, which include:

1. An attractive interaction between electrons can lead to a ground state separated from excited states by an energy gap. The critical field, the thermal properties, and most of the electromagnetic properties are consequences of the energy gap.

2. The electron-lattice-electron interaction leads to an energy gap of the observed magnitude. The indirect interaction proceeds when one electron interacts with the lattice and deforms it; a second electron sees the deformed lattice and adjusts itself to take advantage of the deformation to lower its energy. Thus the second electron interacts with the first electron via the lattice deformation.

3. The penetration depth and the coherence length emerge as natural consequences of the BCS theory. The London equation is obtained for magnetic fields that vary slowly in space. Thus the central phenomenon in superconductivity, the Meissner effect, is obtained in a natural way.

4. The criterion for the transition temperature of an element or alloy involves the electron density of orbitals $D(\epsilon_F)$ of one spin at the Fermi level and the electron-lattice interaction U , which can be estimated from the electrical resistivity because the resistivity at room temperature is a measure of the electron-phonon interaction. For $UD(\epsilon_F) \ll 1$ the BCS theory predicts

$$T_c = 1.14\theta \exp[-1/UD(\epsilon_F)] , \quad (18)$$

where θ is the Debye temperature and U is an attractive interaction. The result for T_c is satisfied at least qualitatively by the experimental data. There is an interesting apparent paradox: the higher the resistivity at room temperature the higher is U , and thus the more likely it is that the metal will be a superconductor when cooled.

5. Magnetic flux through a superconducting ring is quantized and the effective unit of charge is $2e$ rather than e . The BCS ground state involves pairs of electrons; thus flux quantization in terms of the pair charge $2e$ is a consequence of the theory.

BCS Ground State

The filled Fermi sea is the ground state of a Fermi gas of noninteracting electrons. This state allows arbitrarily small excitations—we can form an

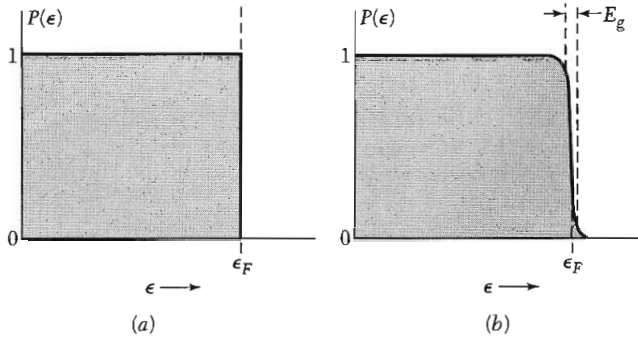


Figure 15 (a) Probability P that an orbital of kinetic energy ϵ is occupied in the ground state of the noninteracting Fermi gas; (b) the BCS ground state differs from the Fermi state in a region of width of the order of the energy gap E_g . Both curves are for absolute zero.

excited state by taking an electron from the Fermi surface and raising it just above the Fermi surface. The BCS theory shows that with an appropriate attractive interaction between electrons the new ground state is superconducting and is separated by a finite energy E_g from its lowest excited state.

The formation of the BCS ground state is suggested by Fig. 15. The BCS state in (b) contains admixtures of one-electron orbitals from above the Fermi energy ϵ_F . At first sight the BCS state appears to have a higher energy than the Fermi state: the comparison of (b) with (a) shows that the kinetic energy of the BCS state is higher than that of the Fermi state. But the attractive potential energy of the BCS state, although not represented in the figure, acts to lower the total energy of the BCS state with respect to the Fermi state.

When the BCS ground state of a many-electron system is described in terms of the occupancy of one-particle orbitals, those near ϵ_F are filled somewhat like a Fermi-Dirac distribution for some finite temperature.

The central feature of the BCS state is that the one-particle orbitals are occupied in pairs: if an orbital with wavevector \mathbf{k} and spin up is occupied, then the orbital with wavevector $-\mathbf{k}$ and spin down is also occupied. If $\mathbf{k}\uparrow$ is vacant, then $-\mathbf{k}\downarrow$ is also vacant. The pairs are called **Cooper pairs**, treated in Appendix H. They have spin zero and have many attributes of bosons.

Flux Quantization in a Superconducting Ring

We prove that the total magnetic flux that passes through a superconducting ring may assume only quantized values, integral multiples of the flux quantum $2\pi\hbar c/q$, where by experiment $q = 2e$, the charge of an electron pair. Flux quantization is a beautiful example of a long-range quantum effect in which the coherence of the superconducting state extends over a ring or solenoid.

Let us first consider the electromagnetic field as an example of a similar boson field. The electric field intensity $E(\mathbf{r})$ acts qualitatively as a probability field amplitude. When the total number of photons is large, the energy density may be written as

$$E^*(\mathbf{r})E(\mathbf{r})/4\pi \cong n(\mathbf{r})\hbar\omega ,$$

where $n(\mathbf{r})$ is the number density of photons of frequency ω . Then we may write the electric field in a semiclassical approximation as

$$E(\mathbf{r}) \cong (4\pi\hbar\omega)^{1/2} n(\mathbf{r})^{1/2} e^{i\theta(\mathbf{r})} \quad E^*(\mathbf{r}) \cong (4\pi\hbar\omega)^{1/2} n(\mathbf{r})^{1/2} e^{-i\theta(\mathbf{r})} ,$$

where $\theta(\mathbf{r})$ is the phase of the field. A similar probability amplitude describes Cooper pairs.

The arguments that follow apply to a boson gas with a large number of bosons in the same orbital. We then can treat the boson probability amplitude as a classical quantity, just as the electromagnetic field is used for photons. Both amplitude and phase are then meaningful and observable. The arguments do not apply to a metal in the normal state because an electron in the normal state acts as a single unpaired fermion that cannot be treated classically.

We first show that a charged boson gas obeys the London equation. Let $\psi(\mathbf{r})$ be the particle probability amplitude. We suppose that the pair concentration $n = \psi^*\psi = \text{constant}$. At absolute zero n is one-half of the concentration of electrons in the conduction band, for n refers to pairs. Then we may write

$$\psi = n^{1/2} e^{i\theta(\mathbf{r})} ; \quad \psi^* = n^{1/2} e^{-i\theta(\mathbf{r})} . \quad (19)$$

The phase $\theta(\mathbf{r})$ is important for what follows. In SI units, set $c = 1$ in the equations that follow.

The velocity of a particle is, from the Hamilton equations of mechanics,

$$\text{(CGS)} \quad \mathbf{v} = \frac{1}{m} \left(\mathbf{p} - \frac{q}{c} \mathbf{A} \right) = \frac{1}{m} \left(-i\hbar\nabla - \frac{q}{c} \mathbf{A} \right) .$$

The particle flux is given by

$$\psi^* \mathbf{v} \psi = \frac{n}{m} \left(\hbar\nabla\theta - \frac{q}{c} \mathbf{A} \right) , \quad (20)$$

so that the electric current density is

$$\mathbf{j} = q\psi^* \mathbf{v} \psi = \frac{nq}{m} \left(\hbar\nabla\theta - \frac{q}{c} \mathbf{A} \right) . \quad (21)$$

We may take the curl of both sides to obtain the London equation:

$$\text{curl } \mathbf{j} = -\frac{nq^2}{mc} \mathbf{B} , \quad (22)$$

with use of the fact that the curl of the gradient of a scalar is identically zero. The constant that multiplies \mathbf{B} agrees with (14a). We recall that the Meissner effect is a consequence of the London equation, which we have here derived.

Quantization of the magnetic flux through a ring is a dramatic consequence of Eq. (21). Let us take a closed path C through the interior of the

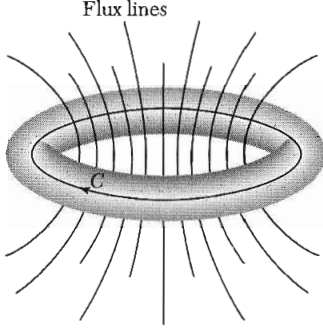


Figure 16 Path of integration C through the interior of a superconducting ring. The flux through the ring is the sum of the flux Φ_{ext} from external sources and the flux Φ_{sc} from the superconducting currents which flow in the surface of the ring; $\Phi = \Phi_{\text{ext}} + \Phi_{\text{sc}}$. The flux Φ is quantized. There is normally no quantization condition on the flux from external sources, so that Φ_{sc} must adjust itself appropriately in order that Φ assume a quantized value.

superconducting material, well away from the surface (Fig. 16). The Meissner effect tells us that \mathbf{B} and \mathbf{j} are zero in the interior. Now (21) is zero if

$$\hbar c \nabla \theta = q \mathbf{A} \quad . \quad (23)$$

We form

$$\oint_C \nabla \theta \cdot d\mathbf{l} = \theta_2 - \theta_1$$

for the change of phase on going once around the ring.

The probability amplitude ψ is measurable in the classical approximation, so that ψ must be single-valued and

$$\theta_2 - \theta_1 = 2\pi s \quad , \quad (24)$$

where s is an integer. By the Stokes theorem,

$$\oint_C \mathbf{A} \cdot d\mathbf{l} = \int_C (\text{curl } \mathbf{A}) \cdot d\boldsymbol{\sigma} = \int_C \mathbf{B} \cdot d\boldsymbol{\sigma} = \Phi \quad , \quad (25)$$

where $d\boldsymbol{\sigma}$ is an element of area on a surface bounded by the curve C , and Φ is the magnetic flux through C . From (23), (24), and (25) we have $2\pi\hbar cs = q\Phi$, or

$$\Phi = (2\pi\hbar c/q)s \quad . \quad (26)$$

Thus the flux through the ring is quantized in integral multiples of $2\pi\hbar c/q$.

By experiment $q = -2e$ as appropriate for electron pairs, so that the quantum of flux in a superconductor is

$$\text{(CGS)} \quad \Phi_0 = 2\pi\hbar c/2e \cong 2.0678 \times 10^{-7} \text{ gauss cm}^2 \quad ;$$

$$\text{(SI)} \quad \Phi_0 = 2\pi\hbar/2e \cong 2.0678 \times 10^{-15} \text{ tesla m}^2 \quad . \quad (27)$$

This flux quantum is called a **fluxoid** or **fluxon**.

The flux through the ring is the sum of the flux Φ_{ext} from external sources and the flux Φ_{sc} from the persistent superconducting currents which flow in

the surface of the ring: $\Phi = \Phi_{\text{ext}} + \Phi_{\text{sc}}$. The flux Φ is quantized. There is normally no quantization condition on the flux from external sources, so that Φ_{sc} must adjust itself appropriately in order that Φ assume a quantized value.

Duration of Persistent Currents

Consider a persistent current that flows in a ring of a type I superconductor of wire of length L and cross-sectional area A . The persistent current maintains a flux through the ring of some integral number of fluxoids (27). A fluxoid cannot leak out of the ring and thereby reduce the persistent current unless by a thermal fluctuation a minimum volume of the superconducting ring is momentarily in the normal state.

The probability per unit time that a fluxoid will leak out is the product

$$P = (\text{attempt frequency})(\text{activation barrier factor}) . \quad (28)$$

The activation barrier factor is $\exp(-\Delta F/k_B T)$, where the free energy of the barrier is

$$\Delta F \approx (\text{minimum volume})(\text{excess free energy density of normal state}) .$$

The minimum volume of the ring that must turn normal to allow a fluxoid to escape is of the order of $R\xi^2$, where ξ is the coherence length of the superconductor and R the wire thickness. The excess free energy density of the normal state is $H_c^2/8\pi$, whence the barrier free energy is

$$\Delta F \approx R\xi^2 H_c^2/8\pi . \quad (29)$$

Let the wire thickness be 10^{-4} cm, the coherence length = 10^{-4} cm, and $H_c = 10^3$ G; then $\Delta F \approx 10^{-7}$ erg. As we approach the transition temperature from below, ΔF will decrease toward zero, but the value given is a fair estimate between absolute zero and $0.8 T_c$. Thus the activation barrier factor is

$$\exp(-\Delta F/k_B T) \approx \exp(-10^8) \approx 10^{-(4.34 \times 10^7)} .$$

The characteristic frequency with which the minimum volume can attempt to change its state must be of the order of E_g/\hbar . If $E_g = 10^{-15}$ erg, the attempt frequency is $\approx 10^{-15}/10^{-27} \approx 10^{12} \text{ s}^{-1}$. The leakage probability (28) becomes

$$P \approx 10^{12} 10^{-4.34 \times 10^7} \text{ s}^{-1} = 10^{-4.34 \times 10^7} \text{ s}^{-1} .$$

The reciprocal of this is a measure of the time required for a fluxoid to leak out, $T = 1/P = 10^{4.34 \times 10^7} \text{ s}$.

The age of the universe is only 10^{18} s, so that a fluxoid will not leak out in the age of the universe, under our assumed conditions. Accordingly, the current is maintained.

There are two circumstances in which the activation energy is much lower and a fluxoid can be observed to leak out of a ring—either very close to the critical temperature, where H_c is very small, or when the material of the ring is

a type II superconductor and already has fluxoids embedded in it. These special situations are discussed in the literature under the subject of fluctuations in superconductors.

Type II Superconductors

There is no difference in the mechanism of superconductivity in type I and type II superconductors. Both types have similar thermal properties at the superconductor-normal transition in zero magnetic field. But the Meissner effect is entirely different (Fig. 5).

A good type I superconductor excludes a magnetic field until superconductivity is destroyed suddenly, and then the field penetrates completely. A good type II superconductor excludes the field completely up to a field H_{c1} . Above H_{c1} the field is partially excluded, but the specimen remains electrically superconducting. At a much higher field, H_{c2} , the flux penetrates completely and superconductivity vanishes. (An outer surface layer of the specimen may remain superconducting up to a still higher field H_{c3} .)

An important difference in a type I and a type II superconductor is in the mean free path of the conduction electrons in the normal state. If the coherence length ξ is longer than the penetration depth λ , the superconductor will be type I. Most pure metals are type I, with $\lambda/\xi < 1$ (see Table 5 on p. 275).

But, when the mean free path is short, the coherence length is short and the penetration depth is great (Fig. 14). This is the situation when $\lambda/\xi > 1$, and the superconductor will be type II.

We can change some metals from type I to type II by a modest addition of an alloying element. In Figure 5 the addition of 2 wt. percent of indium changes lead from type I to type II, although the transition temperature is scarcely changed at all. Nothing fundamental has been done to the electronic structure of lead by this amount of alloying, but the magnetic behavior as a superconductor has changed drastically.

The theory of type II superconductors was developed by Ginzburg, Landau, Abrikosov, and Gorkov. Later Kunzler and co-workers observed that Nb_3Sn wires can carry large supercurrents in fields approaching 100 kG; this led to the commercial development of strong-field superconducting magnets.

Consider the interface between a region in the superconducting state and a region in the normal state. The interface has a surface energy that may be positive or negative and that decreases as the applied magnetic field is increased. A superconductor is type I if the surface energy is always positive as the magnetic field is increased, and type II if the surface energy becomes negative as the magnetic field is increased. The sign of the surface energy has no importance for the transition temperature.

The free energy of a bulk superconductor is increased when the magnetic field is expelled. However, a parallel field can penetrate a very thin film nearly uniformly (Fig. 17), only a part of the flux is expelled, and the energy of the

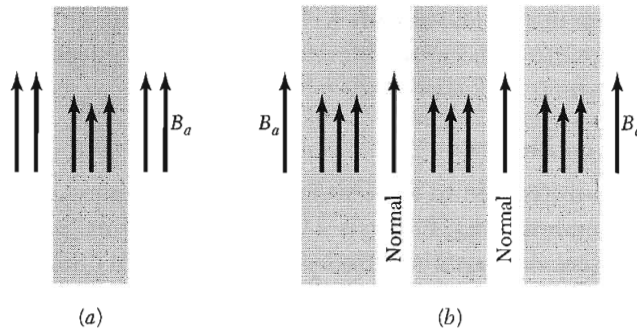


Figure 17 (a) Magnetic field penetration into a thin film of thickness equal to the penetration depth λ . The arrows indicate the intensity of the magnetic field. (b) Magnetic field penetration in a homogeneous bulk structure in the mixed or vortex state, with alternate layers in normal and superconducting states. The superconducting layers are thin in comparison with λ . The laminar structure is shown for convenience; the actual structure consists of rods of the normal state surrounded by the superconducting state. (The N regions in the vortex state are not exactly normal, but are described by low values of the stabilization energy density.)

superconducting film will increase only slowly as the external magnetic field is increased. This causes a large increase in the field intensity required for the destruction of superconductivity. The film has the usual energy gap and will be resistanceless. A thin film is not a type II superconductor, but the film results show that under suitable conditions superconductivity can exist in high magnetic fields.

Vortex State. The results for thin films suggest the question: Are there stable configurations of a superconductor in a magnetic field with regions (in the form of thin rods or plates) in the normal state, each normal region surrounded by a superconducting region? In such a mixed state, called the vortex state, the external magnetic field will penetrate the thin normal regions uniformly, and the field will also penetrate somewhat into the surrounding superconducting material, as in Fig. 18.

The term vortex state describes the circulation of superconducting currents in vortices throughout the bulk specimen, as in Fig. 19. There is no chemical or crystallographic difference between the normal and the superconducting regions in the vortex state. The vortex state is stable when the penetration of the applied field into the superconducting material causes the surface energy to become negative. A type II superconductor is characterized by a vortex state stable over a certain range of magnetic field strength; namely, between H_{c1} and H_{c2} .

Estimation of H_{c1} and H_{c2} . What is the condition for the onset of the vortex state as the applied magnetic field is increased? We estimate H_{c1} from the penetration depth λ . The field in the normal core of the fluxoid will be H_{c1} when the applied field is H_{c1} .

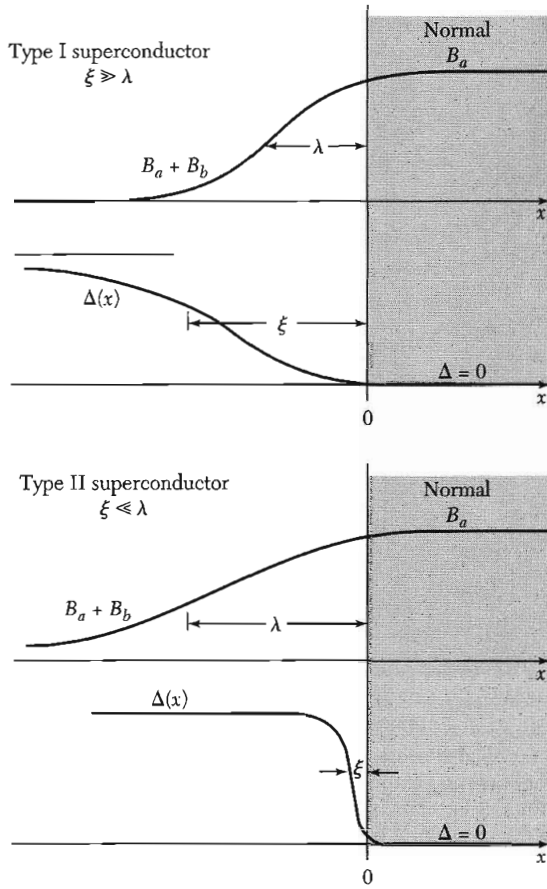


Figure 18 Variation of the magnetic field and energy gap parameter $\Delta(x)$ at the interface of superconducting and normal regions, for type I and type II superconductors. The energy gap parameter is a measure of the stabilization energy density of the superconducting state.

The field will extend out from the normal core a distance λ into the superconducting environment. The flux thus associated with a single core is $\pi\lambda^2 H_{c1}$, and this must be equal to the flux quantum Φ_0 defined by (27). Thus

$$H_{c1} \approx \Phi_0 / \pi\lambda^2 . \tag{30}$$

This is the field for nucleation of a single fluxoid.

At H_{c2} the fluxoids are packed together as tightly as possible, consistent with the preservation of the superconducting state. This means as densely as the coherence length ξ will allow. The external field penetrates the specimen almost uniformly, with small ripples on the scale of the fluxoid lattice. Each core is responsible for carrying a flux of the order of $\pi\xi^2 H_{c2}$, which also is quantized to Φ_0 . Thus

$$H_{c2} \approx \Phi_0 / \pi\xi^2 \tag{31}$$

gives the upper critical field. The larger the ratio λ/ξ , the larger is the ratio of H_{c2} to H_{c1} .

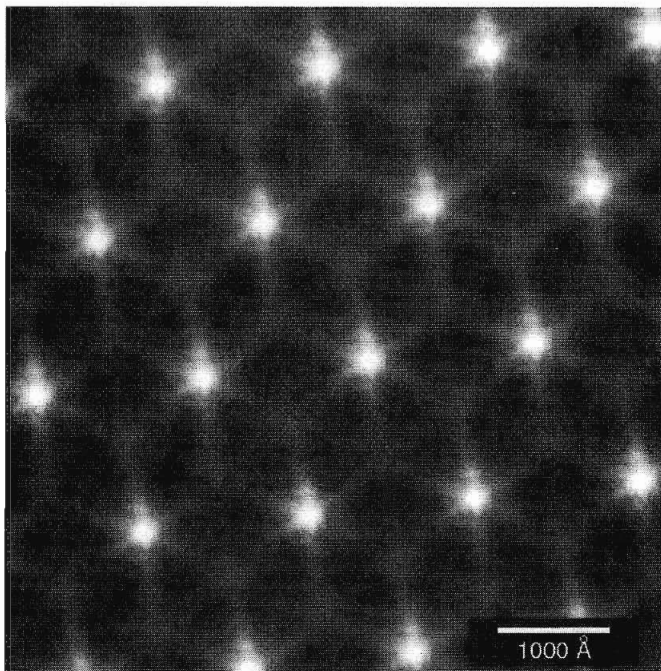


Figure 19 Flux lattice in NbSe_2 at 1,000 gauss at 0.2K, as viewed with a scanning tunneling microscope. The photo shows the density of states at the Fermi level, as in Figure 23. The vortex cores have a high density of states and are shaded white; the superconducting regions are dark, with no states at the Fermi level. The amplitude and spatial extent of these states is determined by a potential well formed by $\Delta(x)$ as in Fig. 18 for a Type II superconductor. The potential well confines the core state wavefunctions in the image here. The star shape is a finer feature, a result special to NbSe_2 of the sixfold disturbance of the charge density at the Fermi surface. Photo courtesy of H. F. Hess.

It remains to find a relation between these critical fields and the thermodynamic critical field H_c that measures the stabilization energy density of the superconducting state, which is known by (9) to be $H_c^2/8\pi$. In a type II superconductor we can determine H_c only indirectly by calorimetric measurement of the stabilization energy. To estimate H_{c1} in terms of H_c , we consider the stability of the vortex state at absolute zero in the impure limit $\xi < \lambda$; here $\kappa > 1$ and the coherence length is short in comparison with the penetration depth.

We estimate in the vortex state the stabilization energy of a fluxoid core viewed as a normal metal cylinder which carries an average magnetic field B_a . The radius is of the order of the coherence length, the thickness of the boundary between N and S phases. The energy of the normal core referred to the energy of a pure superconductor is given by the product of the stabilization energy times the area of the core:

$$\text{(CGS)} \quad f_{\text{core}} \approx \frac{1}{8\pi} H_c^2 \times \pi \xi^2, \quad (32)$$

per unit length. But there is also a decrease in magnetic energy because of the penetration of the applied field B_a into the superconducting material around the core:

$$(CGS) \quad f_{\text{mag}} \approx -\frac{1}{8\pi} B_a^2 \times \pi \lambda^2 . \quad (33)$$

For a single fluxoid we add these two contributions to obtain

$$(CGS) \quad f = f_{\text{core}} + f_{\text{mag}} \approx \frac{1}{8} (H_c^2 \xi^2 - B_a^2 \lambda^2) . \quad (34)$$

The core is stable if $f < 0$. The threshold field for a stable fluxoid is at $f = 0$, or, with H_{c1} written for B_a ,

$$H_{c1}/H_c \approx \xi/\lambda . \quad (35)$$

The threshold field divides the region of positive surface energy from the region of negative surface energy.

We can combine (30) and (35) to obtain a relation for H_c :

$$\pi \xi \lambda H_c \approx \Phi_0 . \quad (36)$$

We can combine (30), (31), and (35) to obtain

$$(H_{c1} H_{c2})^{1/2} \approx H_c , \quad (37a)$$

and

$$H_{c2} \approx (\lambda/\xi) H_c = \kappa H_c . \quad (37b)$$

Single Particle Tunneling

Consider two metals separated by an insulator, as in Fig. 20. The insulator normally acts as a barrier to the flow of conduction electrons from one metal to the other. If the barrier is sufficiently thin (less than 10 or 20 Å) there is a significant probability that an electron which impinges on the barrier will pass from one metal to the other: this is called **tunneling**. In many experiments the insulating layer is simply a thin oxide layer formed on one of two evaporated metal films, as in Fig. 21.

When both metals are normal conductors, the current-voltage relation of the sandwich or tunneling junction is ohmic at low voltages, with the current directly proportional to the applied voltage. Giaever (1960) discovered that if one of the metals becomes superconducting the current-voltage characteristic changes from the straight line of Fig. 22a to the curve shown in Fig. 22b.

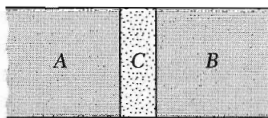


Figure 20 Two metals, A and B, separated by a thin layer of an insulator C.

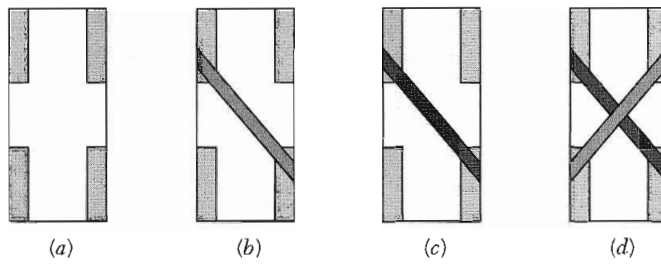


Figure 21 Preparation of an Al/Al₂O₃/Sn sandwich. (a) Glass slide with indium contacts. (b) An aluminum strip 1 mm wide and 1000 to 3000 Å thick has been deposited across the contacts. (c) The aluminum strip has been oxidized to form an Al₂O₃ layer 10 to 20 Å in thickness. (d) A tin film has been deposited across the aluminum film, forming an Al/Al₂O₃/Sn sandwich. The external leads are connected to the indium contacts; two contacts are used for the current measurement and two for the voltage measurement. (After Giaever and Megerle.)

Figure 22 (a) Linear current-voltage relation for junction of normal metals separated by oxide layer; (b) current-voltage relation with one metal normal and the other metal superconducting.

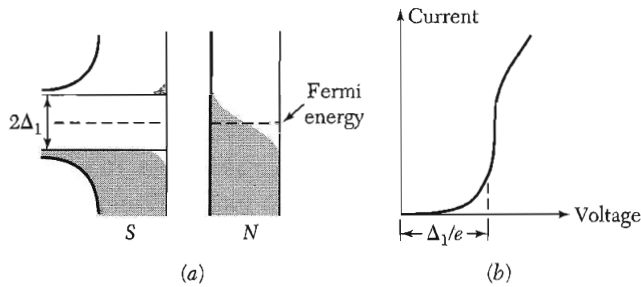
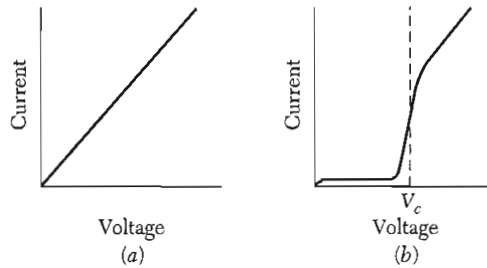


Figure 23 The density of orbitals and the current-voltage characteristic for a tunneling junction. In (a) the energy is plotted on the vertical scale and the density of orbitals on the horizontal scale. One metal is in the normal state and one in the superconducting state. (b) I versus V ; the dashes indicate the expected break at $T = 0$. (After Giaever and Megerle.)

Figure 23a contrasts the electron density of orbitals in the superconductor with that in the normal metal. In the superconductor there is an energy gap centered at the Fermi level. At absolute zero no current can flow until the applied voltage is $V = E_g/2e = \Delta/e$.

The gap E_g corresponds to the break-up of a pair of electrons in the superconducting state, with the formation of two electrons, or an electron and

a hole, in the normal state. The current starts when $eV = \Delta$. At finite temperatures there is a small current flow even at low voltages, because of electrons in the superconductor that are thermally excited across the energy gap.

Josephson Superconductor Tunneling

Under suitable conditions we observe remarkable effects associated with the tunneling of superconducting electron pairs from a superconductor through a layer of an insulator into another superconductor. Such a junction is called a weak link. The effects of pair tunneling include:

Dc Josephson effect. A dc current flows across the junction in the absence of any electric or magnetic field.

Ac Josephson effect. A dc voltage applied across the junction causes rf current oscillations across the junction. This effect has been utilized in a precision determination of the value of \hbar/e . Further, an rf voltage applied with the dc voltage can then cause a dc current across the junction.

Macroscopic long-range quantum interference. A dc magnetic field applied through a superconducting circuit containing two junctions causes the maximum supercurrent to show interference effects as a function of magnetic field intensity. This effect can be utilized in sensitive magnetometers.

Dc Josephson Effect. Our discussion of Josephson junction phenomena follows the discussion of flux quantization. Let ψ_1 be the probability amplitude of electron pairs on one side of a junction, and let ψ_2 be the amplitude on the other side. For simplicity, let both superconductors be identical. For the present we suppose that they are both at zero potential.

The time-dependent Schrödinger equation $i\hbar\partial\psi/\partial t = \mathcal{H}\psi$ applied to the two amplitudes gives

$$i\hbar \frac{\partial\psi_1}{\partial t} = \hbar T\psi_2 ; \quad i\hbar \frac{\partial\psi_2}{\partial t} = \hbar T\psi_1 . \quad (38)$$

Here $\hbar T$ represents the effect of the electron-pair coupling or transfer interaction across the insulator; T has the dimensions of a rate or frequency. It is a measure of the leakage of ψ_1 into the region 2, and of ψ_2 into the region 1. If the insulator is very thick, T is zero and there is no pair tunneling.

Let $\psi_1 = n_1^{1/2} e^{i\theta_1}$ and $\psi_2 = n_2^{1/2} e^{i\theta_2}$. Then

$$\frac{\partial\psi_1}{\partial t} = \frac{1}{2}n_1^{-1/2} e^{i\theta_1} \frac{\partial n_1}{\partial t} + i\psi_1 \frac{\partial\theta_1}{\partial t} = -iT\psi_2 ; \quad (39)$$

$$\frac{\partial\psi_2}{\partial t} = \frac{1}{2}n_2^{-1/2} e^{i\theta_2} \frac{\partial n_2}{\partial t} + i\psi_2 \frac{\partial\theta_2}{\partial t} = -iT\psi_1 . \quad (40)$$

We multiply (39) by $n_1^{1/2} e^{-i\theta_1}$ to obtain, with $\delta \equiv \theta_2 - \theta_1$,

$$\frac{1}{2} \frac{\partial n_1}{\partial t} + in_1 \frac{\partial \theta_1}{\partial t} = -iT(n_1 n_2)^{1/2} e^{i\delta} . \quad (41)$$

We multiply (40) by $n_2^{1/2} e^{-i\theta_2}$ to obtain

$$\frac{1}{2} \frac{\partial n_2}{\partial t} + in_2 \frac{\partial \theta_2}{\partial t} = -iT(n_1 n_2)^{1/2} e^{-i\delta} . \quad (42)$$

Now equate the real and imaginary parts of (41) and similarly of (42):

$$\frac{\partial n_1}{\partial t} = 2T(n_1 n_2)^{1/2} \sin \delta ; \quad \frac{\partial n_2}{\partial t} = -2T(n_1 n_2)^{1/2} \sin \delta ; \quad (43)$$

$$\frac{\partial \theta_1}{\partial t} = -T \left(\frac{n_2}{n_1} \right)^{1/2} \cos \delta ; \quad \frac{\partial \theta_2}{\partial t} = -T \left(\frac{n_1}{n_2} \right)^{1/2} \cos \delta . \quad (44)$$

If $n_1 \equiv n_2$ as for identical superconductors 1 and 2, we have from (44) that

$$\frac{\partial \theta_1}{\partial t} = \frac{\partial \theta_2}{\partial t} ; \quad \frac{\partial}{\partial t} (\theta_2 - \theta_1) = 0 . \quad (45)$$

From (43) we see that

$$\frac{\partial n_2}{\partial t} = -\frac{\partial n_1}{\partial t} . \quad (46)$$

The current flow from (1) to (2) is proportional to $\partial n_2 / \partial t$ or, the same thing, $-\partial n_1 / \partial t$. We therefore conclude from (43) that the current J of superconductor pairs across the junction depends on the phase difference δ as

$$J = J_0 \sin \delta = J_0 \sin (\theta_2 - \theta_1) . \quad (47)$$

where J_0 is proportional to the transfer interaction T . The current J_0 is the maximum zero-voltage current that can be passed by the junction. With no applied voltage a dc current will flow across the junction (Fig. 24), with a value between J_0 and $-J_0$ according to the value of the phase difference $\theta_2 - \theta_1$. This is the **dc Josephson effect**.

Ac Josephson Effect. Let a dc voltage V be applied across the junction. We can do this because the junction is an insulator. An electron pair experiences a potential energy difference qV on passing across the junction, where $q = -2e$. We can say that a pair on one side is at potential energy $-eV$ and a pair on the other side is at eV . The equations of motion that replace (38) are

$$i\hbar \partial \psi_1 / \partial t = \hbar T \psi_2 - eV \psi_1 ; \quad i\hbar \partial \psi_2 / \partial t = \hbar T \psi_1 + eV \psi_2 . \quad (48)$$

We proceed as above to find in place of (41) the equation

$$\frac{1}{2} \frac{\partial n_1}{\partial t} + in_1 \frac{\partial \theta_1}{\partial t} = ieV n_1 \hbar^{-1} - iT(n_1 n_2)^{1/2} e^{i\delta} . \quad (49)$$

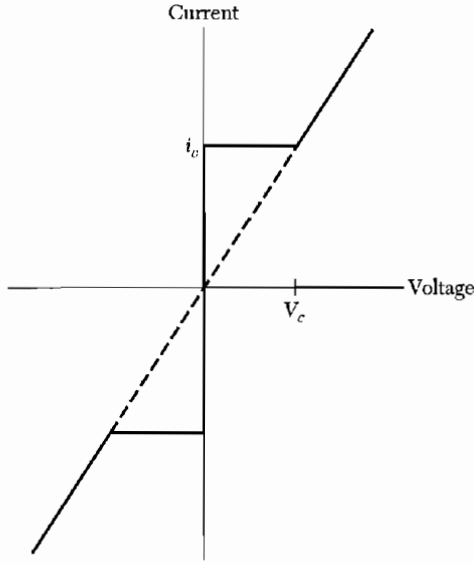


Figure 24 Current-voltage characteristic of a Josephson junction. Dc currents flow under zero applied voltage up to a critical current i_c ; this is the dc Josephson effect. At voltages above V_c the junction has a finite resistance, but the current has an oscillatory component of frequency $\omega = 2eV/\hbar$; this is the ac Josephson effect.

This equation breaks up into the real part

$$\partial n_1/\partial t = 2T(n_1 n_2)^{1/2} \sin \delta , \quad (50)$$

exactly as without the voltage V , and the imaginary part

$$\partial \theta_1/\partial t = (eV/\hbar) - T(n_2/n_1)^{1/2} \cos \delta , \quad (51)$$

which differs from (44) by the term eV/\hbar .

Further, by extension of (42),

$$\frac{1}{2} \frac{\partial n_2}{\partial t} + in_2 \frac{\partial \theta_2}{\partial t} = -i eV n_2 \hbar^{-1} - iT(n_1 n_2)^{1/2} e^{-i\delta} , \quad (52)$$

whence

$$\partial n_2/\partial t = -2T(n_1 n_2)^{1/2} \sin \delta ; \quad (53)$$

$$\partial \theta_2/\partial t = -(eV/\hbar) - T(n_1/n_2)^{1/2} \cos \delta . \quad (54)$$

From (51) and (54) with $n_1 \cong n_2$, we have

$$\partial(\theta_2 - \theta_1)/\partial t = \partial \delta/\partial t = -2eV/\hbar . \quad (55)$$

We see by integration of (55) that with a dc voltage across the junction the relative phase of the probability amplitudes varies as

$$\delta(t) = \delta(0) - (2eVt/\hbar) . \quad (56)$$

The superconducting current is given by (47) with (56) for the phase:

$$J = J_0 \sin [\delta(0) - (2eVt/\hbar)] . \quad (57)$$

The current oscillates with frequency

$$\omega = 2eV/\hbar . \quad (58)$$

This is the **ac Josephson effect**. A dc voltage of $1 \mu\text{V}$ produces a frequency of 483.6 MHz. The relation (58) says that a photon of energy $\hbar\omega = 2eV$ is emitted or absorbed when an electron pair crosses the barrier. By measuring the voltage and the frequency it is possible to obtain a very precise value of e/\hbar .

Macroscopic Quantum Interference. We saw in (24) and (26) that the phase difference $\theta_2 - \theta_1$ around a closed circuit which encompasses a total magnetic flux Φ is given by

$$\theta_2 - \theta_1 = (2e/\hbar c)\Phi . \quad (59)$$

The flux is the sum of that due to external fields and that due to currents in the circuit itself.

We consider two Josephson junctions in parallel, as in Fig. 25. No voltage is applied. Let the phase difference between points 1 and 2 taken on a path through junction a be δ_a . When taken on a path through junction b , the phase difference is δ_b . In the absence of a magnetic field these two phases must be equal.

Now let the flux Φ pass through the interior of the circuit. We do this with a straight solenoid normal to the plane of the paper and lying inside the circuit. By (59), $\delta_b - \delta_a = (2e/\hbar c)\Phi$, or

$$\delta_b = \delta_0 + \frac{e}{\hbar c} \Phi ; \quad \delta_a = \delta_0 - \frac{e}{\hbar c} \Phi . \quad (60)$$

The total current is the sum of J_a and J_b . The current through each junction is of the form (47), so that

$$J_{\text{Total}} = J_0 \left\{ \sin \left(\delta_0 + \frac{e}{\hbar c} \Phi \right) + \sin \left(\delta_0 - \frac{e}{\hbar c} \Phi \right) \right\} = 2(J_0 \sin \delta_0) \cos \frac{e\Phi}{\hbar c} .$$

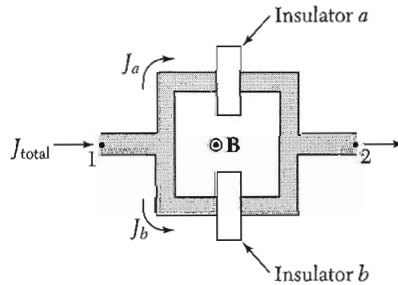


Figure 25 The arrangement for experiment on macroscopic quantum interference. A magnetic flux Φ passes through the interior of the loop.

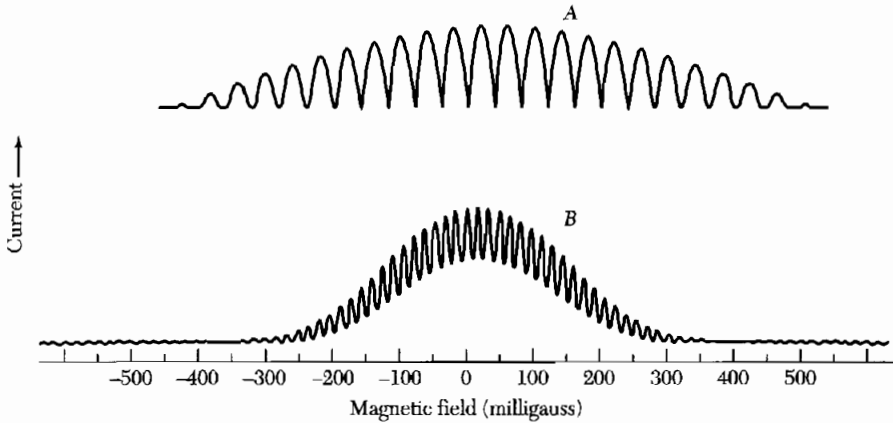


Figure 26 Experimental trace of J_{\max} versus magnetic field showing interference and diffraction effects for two junctions A and B. The field periodicity is 39.5 and 16 mG for A and B, respectively. Approximate maximum currents are 1 mA (A) and 0.5 mA (B). The junction separation is 3 mm and junction width 0.5 mm for both cases. The zero offset of A is due to a background magnetic field. (After R. C. Jaklevic, J. Lambe, J. E. Mercereau, and A. H. Silver.)

The current varies with Φ and has maxima when

$$e\Phi/\hbar c = s\pi, \quad s = \text{integer}. \quad (61)$$

The periodicity of the current is shown in Fig. 26. The short period variation is produced by interference from the two junctions, as predicted by (61). The longer period variation is a diffraction effect and arises from the finite dimensions of each junction—this causes Φ to depend on the particular path of integration (Problem 6).

HIGH-TEMPERATURE SUPERCONDUCTORS

High T_c or HTS denotes superconductivity in materials, chiefly copper oxides, with high transition temperatures, accompanied by high critical currents and magnetic fields. By 1988 the long-standing 23 K ceiling of T_c in intermetallic compounds had been elevated to 125 K in bulk superconducting oxides; these passed the standard tests for superconductivity—the Meissner effect, ac Josephson effect, persistent currents of long duration, and substantially zero dc resistivity. Memorable steps in the advance include:

$\text{BaPb}_{0.75}\text{Bi}_{0.25}\text{O}_3$	$T_c = 12 \text{ K}$	[BPBO]
$\text{La}_{1.85}\text{Ba}_{0.15}\text{CuO}_4$	$T_c = 36 \text{ K}$	[LBCO]
$\text{YBa}_2\text{Cu}_3\text{O}_7$	$T_c = 90 \text{ K}$	[YBCO]
$\text{Tl}_2\text{Ba}_2\text{Ca}_2\text{Cu}_3\text{O}_{10}$	$T_c = 120 \text{ K}$	[TBCO]
$\text{Hg}_{0.9}\text{Tl}_{0.2}\text{Ba}_2\text{Ca}_2\text{Cu}_3\text{O}_{8.33}$	$T_c = 138 \text{ K}$	

SUMMARY
(In CGS Units)

- A superconductor exhibits infinite conductivity.
- A bulk specimen of metal in the superconducting state exhibits perfect diamagnetism, with the magnetic induction $\mathbf{B} = 0$. This is the Meissner effect. The external magnetic field will penetrate the surface of the specimen over a distance determined by the penetration depth λ .
- There are two types of superconductors, I and II. In a bulk specimen of type I superconductor the superconducting state is destroyed and the normal state is restored by application of an external magnetic field in excess of a critical value H_c . A type II superconductor has two critical fields, $H_{c1} < H_c < H_{c2}$; a vortex state exists in the range between H_{c1} and H_{c2} . The stabilization energy density of the pure superconducting state is $H_c^2/8\pi$ in both type I and II superconductors.
- In the superconducting state an energy gap, $E_g \approx 4k_B T_c$, separates superconducting electrons below from normal electrons above the gap. The gap is detected in experiments on heat capacity, infrared absorption, and tunneling.
- Three important lengths enter the theory of superconductivity; the London penetration depth λ_L ; the intrinsic coherence length ξ_0 ; and the normal electron mean free path ℓ .
- The London equation

$$\mathbf{j} = -\frac{c}{4\pi\lambda_L^2}\mathbf{A} \quad \text{or} \quad \text{curl } \mathbf{j} = -\frac{c}{4\pi\lambda_L^2}\mathbf{B}$$

leads to the Meissner effect through the penetration equation $\nabla^2 B = B/\lambda_L^2$, where $\lambda_L \approx (mc^2/4\pi ne^2)^{1/2}$ is the London penetration depth.

- In the London equation \mathbf{A} or \mathbf{B} should be a weighted average over the coherence length ξ . The intrinsic coherence length $\xi_0 = 2\hbar v_F/\pi E_g$.
- The BCS theory accounts for a superconducting state formed from pairs of electrons $\mathbf{k}\uparrow$ and $-\mathbf{k}\downarrow$. These pairs act as bosons.
- Type II superconductors have $\xi < \lambda$. The critical fields are related by $H_{c1} \approx (\xi/\lambda)H_c$ and $H_{c2} \approx (\lambda/\xi)H_c$. The Ginzburg-Landau parameter κ is defined as λ/ξ .

Problems

1. **Magnetic field penetration in a plate.** The penetration equation may be written as $\lambda^2 \nabla^2 B = B$, where λ is the penetration depth. (a) Show that $B(x)$ inside a superconducting plate perpendicular to the x axis and of thickness δ is given by

$$B(x) = B_a \frac{\cosh(x/\lambda)}{\cosh(\delta/2\lambda)},$$

where B_a is the field outside the plate and parallel to it; here $x = 0$ is at the center of the plate. (b) The effective magnetization $M(x)$ in the plate is defined by $B(x) - B_a = 4\pi M(x)$. Show that, in CGS, $4\pi M(x) = -B_a(1/8\lambda^2)(\delta^2 - 4x^2)$, for $\delta \ll \lambda$. In SI we replace the 4π by μ_0 .

2. **Critical field of thin films.** (a) Using the result of Problem 1b, show that the free energy density at $T = 0$ K within a superconducting film of thickness δ in an external magnetic field B_a is given by, for $\delta \ll \lambda$,

$$\text{(CGS)} \quad F_S(x, B_a) = U_S(0) + (\delta^2 - 4x^2)B_a^2/64\pi\lambda^2 .$$

In SI the factor π is replaced by $\frac{1}{4}\mu_0$. We neglect a kinetic energy contribution to the problem. (b) Show that the magnetic contribution to F_S when averaged over the thickness of the film is $B_a^2(\delta/\lambda)^2/96\pi$. (c) Show that the critical field of the thin film is proportional to $(\lambda/\delta)H_c$, where H_c is the bulk critical field, if we consider only the magnetic contribution to U_S .

3. **Two-fluid model of a superconductor.** On the two-fluid model of a superconductor we assume that at temperatures $0 < T < T_c$ the current density may be written as the sum of the contributions of normal and superconducting electrons: $\mathbf{j} = \mathbf{j}_N + \mathbf{j}_S$, where $\mathbf{j}_N = \sigma_0\mathbf{E}$ and \mathbf{j}_S is given by the London equation. Here σ_0 is an ordinary normal conductivity, decreased by the reduction in the number of normal electrons at temperature T as compared to the normal state. Neglect inertial effects on both j_N and j_S . (a) Show from the Maxwell equations that the dispersion relation connecting wavevector \mathbf{k} and frequency ω for electromagnetic waves in the superconductor is

$$\text{(CGS)} \quad k^2c^2 = 4\pi\sigma_0\omega i - c^2\lambda_L^{-2} + \omega^2 ; \quad \text{or}$$

$$\text{(SI)} \quad k^2c^2 = (\sigma_0/\epsilon_0)\omega i - c^2\lambda_L^{-2} + \omega^2 ;$$

where λ_L^2 is given by (14a) with n replaced by n_s . Recall that $\text{curl curl } \mathbf{B} = -\nabla^2\mathbf{B}$. (b) If τ is the relaxation time of the normal electrons and n_N is their concentration, show by use of the expression $\sigma_0 = n_N e^2 \tau / m$ that at frequencies $\omega \ll 1/\tau$ the dispersion relation does not involve the normal electrons in an important way, so that the motion of the electrons is described by the London equation alone. The supercurrent short-circuits the normal electrons. The London equation itself only holds true if $\hbar\omega$ is small in comparison with the energy gap. Note: The frequencies of interest are such that $\omega \ll \omega_p$, where ω_p is the plasma frequency.

- *4. **Structure of a vortex.** (a) Find a solution to the London equation that has cylindrical symmetry and applies outside a line core. In cylindrical polar coordinates, we want a solution of

$$B - \lambda^2 \nabla^2 B = 0$$

*This problem is somewhat difficult.

that is singular at the origin and for which the total flux is the flux quantum:

$$2\pi \int_0^{\infty} d\rho \rho B(\rho) = \Phi_0 .$$

The equation is in fact valid only outside the normal core of radius ξ . (b) Show that the solution has the limits

$$B(\rho) \approx (\Phi_0/2\pi\lambda^2) \ln(\lambda/\rho) , \quad (\xi \ll \rho \ll \lambda)$$

$$B(\rho) \approx (\Phi_0/2\pi\lambda^2)(\pi\lambda/2\rho)^{1/2} \exp(-\rho/\lambda) . \quad (\rho \gg \lambda)$$

5. **London penetration depth.** (a) Take the time derivative of the London equation (10) to show that $\partial \mathbf{j}/\partial t = (c^2/4\pi\lambda_L^2)\mathbf{E}$. (b) If $m d\mathbf{v}/dt = q\mathbf{E}$, as for free carriers of charge q and mass m , show that $\lambda_L^2 = mc^2/4\pi nq^2$.
6. **Diffraction effect of Josephson junction.** Consider a junction of rectangular cross section with a magnetic field B applied in the plane of the junction, normal to an edge of width w . Let the thickness of the junction be T . Assume for convenience that the phase difference of the two superconductors is $\pi/2$ when $B = 0$. Show that the dc current in the presence of the magnetic field is

$$J \approx J_0 \frac{\sin(wTB_e/\hbar c)}{(wTB_e/\hbar c)} .$$

7. **Meissner effect in sphere.** Consider a sphere of a type I superconductor with critical field H_c . (a) Show that in the Meissner regime the effective magnetization M within the sphere is given by $-8\pi M/3 = B_a$, the uniform applied magnetic field. (b) Show that the magnetic field at the surface of the sphere in the equatorial plane is $3B_a/2$. (It follows that the applied field at which the Meissner effect starts to break down is $2H_c/3$.) Reminder: The demagnetization field of a uniformly magnetized sphere is $-4\pi M/3$.

Reference

An excellent superconductor review is the website superconductors.org.